BULLETIN OF BIOMATHEMATICS

Bulletin of Biomathematics, 2025, 3(2), 111–149

https://dergipark.org.tr/en/pub/bulletinbiomath
ISSN Online: 2980-1869 / Open Access
https://doi.org/10.59292/bulletinbiomath.1664603

REVIEW ARTICLE

Around the brain in 80 Hz: A Kuramoto model perspective of cortical neuronal activity

Aran Dabbaghchi [1,2,*,‡] and **Stuart Townley** [1,2,‡]

[1]Centre for Environmental Mathematics, Faculty of Environment, Science and Economy, University of Exeter, Penryn, TR10 9FE Cornwall, United Kingdom, [2]Environment & Sustainability Institute, University of Exeter, Penryn, TR10 9FE Cornwall, United Kingdom

* Corresponding Author
‡ ad1122@exeter.ac.uk (Aran Dabbaghchi); s.b.townley@exeter.ac.uk (Stuart Townley)

Abstract

Understanding the collective behaviour of cortical neurons is a significant subject, especially in unravelling brain function and dysfunction, specifically in neural disorders. The Kuramoto model is a mathematical framework that allows us to study synchronization patterns in coupled oscillators and explore the underlying dynamics. In this review, we examine the evolution and application of this model to cortical neural activity, focusing on extensions and variants that capture complex phenomena. We trace the development of the Kuramoto model from Winfree's foundational works to the recent forms, including stochastic, second-order, and multi-population variants. Key findings highlight the ability of the model to represent phase transitions from incoherence to synchrony, driven by coupling strength, and its reductions from the high-dimensional form via techniques like the Ott-Antonsen ansatz. Regarding brain disorders, the model shows how excessive synchronization underlies Parkinsonian motor deficits and epileptic seizures, with adaptations such as contrarian nodes and dynamic couplings providing information on desynchronizations. Analytical and numerical results demonstrate critical thresholds and order parameters that determine coherence states that align with empirical data. Extensions of the model clarify the mechanisms that trigger neural disorders and suggest therapeutic methods such as control and optimisation of deep-brain stimulation. Prospective work can refine these models by considering a more realistic network topology and adding noise effect terms, enhancing the predictive and practical power for clinical interventions.

Keywords: Kuramoto model; neural synchronization; cortical activity; brain neural disorders
AMS 2020 Classification: 37N25; 93C10; 92B20; 34C15

1 Introduction

Synchronization has always been an intriguing phenomenon that has occupied mathematicians and scientists. From the 17th century, when Huygens proposed the question of how two syn-

➤ **Received:** 07.04.2025 ➤ **Revised:** 14.05.2025 ➤ **Accepted:** 22.05.2025 ➤ **Published:** 31.10.2025

chronous clockworks interact with each other, to the contributions of Appleton and Van der Pol in the 20th century and up to the current issues in this field, it has always been an important topic for a variety of researchers. A recent trend in the field is the focus on neuronal activities and corresponding dynamics. Neurons communicate with each other to transmit messages and trigger brain commands. Most of these neuronal communications involve some kind of synchronization pattern. This leads to the crucial role of pattern formation, spiking activity, and types of possible connections between neurons. A wealth of useful theories and models have been developed over the last 70 years, from the Hodgkin-Huxley conductance-based model to Winfree's synchronization model. One of the most appealing models is the Kuramoto model, introduced by the Japanese physicist Yoshiki Kuramoto in 1975. This is a mathematically tractable model that can be reshaped in many ways because of its simplicity and flexibility. In this paper, our intention is to review a number of ideas on the Kuramoto model and its profound applications in neural activities, ranging from mathematical to fully applied and practical approaches. The review is organised in three main parts.

The first part consists of the study of the Kuramoto model from a mathematical point of view. We introduce the model, discuss its history, and report some analyses, including: the interpretation of the individual synchronization states; the analysis of the mean field; the analysis of self-consistency; and reduction methods. Finally, we briefly introduce some variants of the Kuramoto model, such as the stochastic Kuramoto model and the second-order model. In this part, we hope to have given the reader a theoretical insight into the Kuramoto model and its background.

The second part is devoted to neuronal activities. This part attempts to present the performance of the Kuramoto model as a basic model to study various types of synchrony and asynchrony in terms of network architecture, excitatory-inhibitory behaviour, modular and regional interactions, and excessive synchronizations. At this point, a link is made between the functionality of the Kuramoto model and the prevailing neuronal activities and phenomena. Basically, it answers the question: "What is going on in a neuronal network in the brain?"

In the third and final part, we consider two well-known neuronal disorders – Parkinson's disease and epilepsy – that are global health problems. It is exciting to see to what extent the Kuramoto model can help us to study how neuronal synchronization and desynchronization arise in these disorders. Indeed, these brain disorders are the direct result of changes in the synchronization pattern. We also review some recently published results that show how the Kuramoto model can help us treat, or at least control and suppress the symptoms. A hot topic in treatment of such disorders, that has attracted much attention, is deep brain stimulation (DBS). DBS has been studied using the Kuramoto model, both for the effects of DBS and in the context of the topological features of the oscillator network and the corresponding design of the DBS nodes.

The review concludes with a brief discussion of our own ideas and some future possible research on how Kuramoto modelling may help improve the treatment and suppression of brain disorders.

2 Mathematical background of the Kuramoto model

Due to the importance of understanding the collective behaviour of coupled oscillators in natural phenomena, numerous theoretical ideas have been proposed in the form of dynamical models. One of the first studies of collective synchronisation was conducted by Winfree in the late 1960*s* when he proposed his mathematical model (1) based on Fourier integrals [1, 2]. Winfree's approach focused mainly on the interactions between limit cycle oscillators in large populations. He intuitively recognized weakly coupled identical oscillators, so-called *relaxation oscillations* [2], analysing their dynamics by separating the time scales, one fast and one slow. Winfree presented

a model in the form:

$$\dot{\theta}_i = \omega_i + \left(\sum_{j=1}^{N} X(\theta_j) \right) Z(\theta_j), \quad j = 1, 2, 3, ..., N, \tag{1}$$

where θ_i and ω_i denote the phase and natural frequency of oscillator i, respectively [1]. In addition, for each oscillator there is a kind of phase-dependent influence $X(\theta_i)$ on the entire population as well as a phase-dependent response function $Z(\theta_i)$ for oscillators. This early experimental work by Winfree led Kuramoto to think further about this model and also about the corresponding natural phenomenon. Together with Nishikawa, Kuramoto started working on this topic in 1975 and published their first theory in [3]. This paper explained some key ideas and, more fundamentally, introduced the revolutionary Kuramoto model. A few years later, in the mid-1980s, Kuramoto further developed the analysis taking into account the intuition given by Winfree and used perturbation techniques to prove that, under assumptions from Winfree's approach, the long-term dynamic behaviour of limit cycle oscillators can be characterised in the following form [2, 4]:

$$\dot{\theta}_i = \omega_i + \sum_{j=1}^{N} \Gamma_{ij}(\theta_j - \theta_i), \ i = 1, 2, 3, ..., N. \tag{2}$$

Where Γ_{ij} is the *coupling* or better to say the *interaction function*. The main problem in the Kuramoto and Winfree approaches was the difficulty of analysis in spite of significant simplifications. This was due to the existence of many arbitrary Fourier harmonics in the coupling functions and the unspecified topology of the network [2]. The classical Kuramoto model is in fact the simplest possible case when considering the same strength of coupling between the oscillators in the form of a fully connected and purely sinusoidal network:

$$\Gamma_{ij}(\theta_j - \theta_i) = \frac{K}{N} \sin(\theta_j - \theta_i).$$

Where $K \geq 0$ is the coupling strength and $\frac{1}{N}$ is the normalization factor as $N \to \infty$. In Kuramoto's approach, the natural frequencies are selected from some distribution $g(\omega)$. To facilitate analysis, Kuramoto assumed that $g(\omega)$ is *unimodal* and *symmetric* about a mean frequency Ω – [2, 3]. Based on the *rotating frame* technique in synchronisation theory, it is possible to shift the phases $\theta_i \to \theta_i + \Omega t$ for all nodes to set the mean frequency Ω equal to zero. This leads to a governing equation:

$$\dot{\theta}_i = \Omega_i + \frac{K}{N} \sum_{j=1}^{N} \sin(\theta_j - \theta_i). \tag{3}$$

An attractive feature of the Kuramoto model (3) is that it is tractable despite the high dimensionality, nonlinearity, and randomness! Moreover, the underlying collective behaviour shows sudden transitions of oscillation from incoherent to ordered [5]. This occurs through an abrupt synchronisation after exceeding certain critical threshold values of the coupling strength.

A source of attraction

An immediate and intriguing phenomenon that results from the simple structure of the Kuramoto model is the potential attraction between oscillators. Indeed, consider any two oscillators i and j

and suppose that one of them, j say, is slightly ahead of a second oscillator, i say, meaning their phase difference $\theta_j - \theta_i$ is positive. Then $\sin(\theta_j - \theta_i)$ is also positive, and multiplying by a positive coupling strength $K \geq 0$, the resulting product $K \sin(\theta_j - \theta_i)$ is also positive. In turn, this makes a positive contribution to the phase velocity of the i^{th} oscillator, forcing the i^{th} oscillator to catch up with the j^{th} oscillator.

Normalization factor

There has been a great deal of focus on the collective behaviour of the Kuramoto model with large populations of size $N >> 1$. If the coupling functions of all oscillators take on positive values, then the sum of them will grow in proportion to N. To prevent unboundedness and so have a well-behaved system, it is necessary to introduce a normalization factor $\frac{1}{N}$ to regulate the coupling term [5].

Order parameter

Let us consider each oscillator's phase as an argument for a complex number of magnitudes equal to one. This complex number can be written as:

$$x + iy = \cos(\theta_i) + i \sin(\theta_i) = e^{i\theta_i}.$$

With this complex number representation of phases, we then define r and ψ by

$$re^{i\psi} = \frac{1}{N} \sum_{j=1}^{N} e^{i\theta_j}, \tag{4}$$

where $0 \leq r \leq 1$ is the radius, while the complex-valued quantity $e^{i\psi}$ is called the *complex order parameter*.

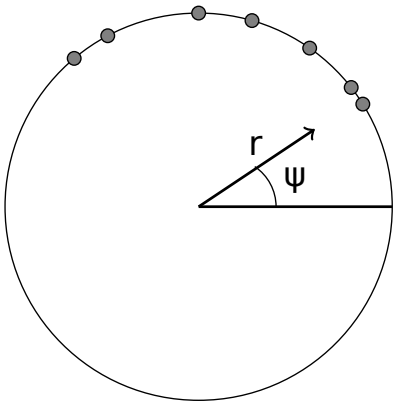

Figure 1. Schematic diagram of phase oscillators

As can be seen in Figure 1, this order parameter is the geometric centroid of the oscillators in their complex number representation. The parameter r measures the level of phase coherence in the oscillators' population. The angular parameter ψ is also the averaged phase of the system. If $r = 1$, then we see complete coherence between the oscillators. In this case, all oscillators have the same

phase, ϕ say, and then $e^{i\theta_j} = e^{i\phi}$ for all oscillators θ_j, and we have:

$$re^{i\psi} = \frac{1}{N}\sum_{i=1}^{N} e^{i\theta_i} = \frac{1}{N}\sum_{i=1}^{N} e^{i\phi} = e^{i\phi}.$$

At the other extreme, if there is no coherence (complete incoherence), then $r = 0$. This means that the complex numbers $e^{i\theta_j}$ are as far out of phase as possible. In this case, each oscillator sits on the vertices of a regular N-gon centred at the origin of the circle. By symmetry, the centroid of the vertices must coincide with the centre of the polygon and therefore $r = 0$ [5].
In the (almost) coherent case, with $r = 1$ (or at least $r \approx 1$), all (almost all) oscillators move in a single cluster. In contrast, in the (almost) incoherent case, with $r = 0$ ($r \approx 0$), all (almost all) phases of the oscillators are distributed as individual points around the circle and move incoherently.
Several questions arise. What is the role of K in the Kuramoto model? How can we vary the coupling strength until we find some information about the coherence status of the system? To explore the evolution of the order parameter, Strogatz [2, 5] ran a simulation with $N = 1000$ oscillators, coupling strength $K = 1$, and a Gaussian distribution for the natural frequencies. At first $r = 1$, but after a period of time, r reduces from $r = 1$, eventually bouncing close to $r = 0$. This means that the system loses its initial coherence and gradually falls to incoherence, as if $K = 0$. This is due to the low level of coupling strength, which means that $K = 1$ is not powerful enough to preserve the complete coherence of the system. The observed fluctuations close to the incoherent state $r = 0$ are caused by the finite number in the population. This effect is known as a **finite size effect** (see Figure 2). In contrast, if we allow the system to have infinitely many oscillators $(N \to \infty)$, then these fluctuations will disappear and $r(t)$ will smoothly approach $r = 0$. Mathematically speaking, the size of the fluctuations is proportional to $\frac{1}{\sqrt{N}}$, which tends to zero as $N \to \infty$ [3, 5].

Mean-field theory in infinite systems

As observed above, $r(t)$ tends to approach some constant level. In the finite N case, there are inversely proportional fluctuations in size to $\sqrt{N}$, the square root of the population. As N tends to infinity, the fluctuations disappear. Kuramoto guessed that $r(t)$ always has some constant asymptotic limits. This extraordinary conjecture was contradictory to the behaviour of many other well-known systems, such as the Lorenz system. Inspiration or luck, Kuramoto was right – for infinitely many populations, the order parameter becomes constant in the long term. Considering a symmetric unimodal distribution function $g(\omega)$, Kuramoto showed that the limiting value of the order parameter (r_∞) depends on K, but remarkably, the system does not become more ordered by increasing K. Instead, the order parameter is zero below a nonzero critical value, (K_c), of the coupling strength. Suddenly, upon reaching this critical value, a phase transition occurs and the whole system self-sustains itself in some kind of coherent state with $r_\infty(K) > 0$. Technically, this means that below the critical value, the oscillators move as if they are uncoupled, and they are uniformly distributed around the circle. In this case, the order parameter descends to a tiny value close to zero and some fluctuations can be observed in the case of finite N. On the other hand, when K exceeds its critical value, the dynamics change their behaviour and the oscillators become ordered or, in other words, act in a coherent state. This happens when the incoherent state becomes unstable and $r(t)$ increases exponentially, emerging as a synchronized cluster of phase oscillators. The asymptotic limit $r_\infty(K)$ is less than 1 (complete coherence) [3, 4]. Usually, based on the type of distribution of the natural frequencies, the shape of the ordering might change. However, in general those oscillators with natural frequencies from central regions of the distribution, closer

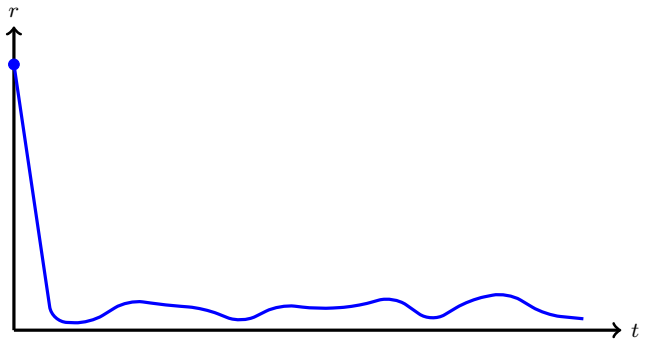

Figure 2. Finite size effect

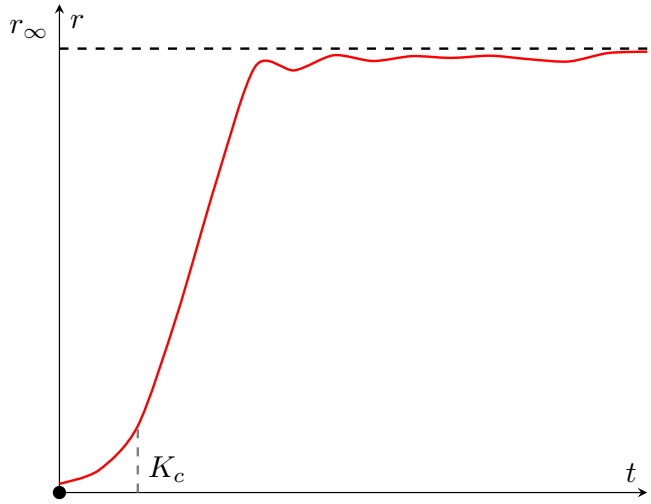

Figure 3. Critical value of K_c and the order parameter's asymptotic limit

to the mode, eventually shape a phase-locked cluster and oscillate in a group. The ones with natural frequencies from the extremities of the distribution, known as the tails of the distribution, commonly run with their own frequency and somehow tend to drift relative to the phase-locked cohort. This situation is commonly termed partially synchronized [2]. By increasing the coupling strength more and more, independent oscillators will join the club of ordered oscillators, and r_∞ will grow. Taking a look at the Kuramoto model, we can see that the coupling term can be reformulated as some new expression in terms of $r(t)$ and ψ, basically by using the complex order parameter $re^{i\psi} = \frac{1}{N}\sum_{j=1}^{N} e^{i\theta_j}$. Multiplying by $e^{-i\theta_i}$ gives:

$$re^{i(\psi-\theta_i)} = \frac{1}{N}\sum_{j=1}^{N} e^{i(\theta_j-\theta_i)}.$$

Considering only the imaginary part, we have the following:

$$r\sin(\psi-\theta_i) = \frac{1}{N}\sum_{j=1}^{N}\sin(\theta_j-\theta_i),$$

hence, the original model will be:

$$\dot{\theta}_i = \omega_i + Kr\sin(\psi-\theta_i).$$

This tells some important stories; the oscillations depend only on the average quantities ψ and r. In fact, this is simply the *mean-field coupling* [5]. Next, we can use the symmetry of the Kuramoto model, by allowing the oscillations frame to rotate at some constant frequencies. The governing equation remains the same; so, by shifting the frequencies of the oscillators, we can neutralize this effect. Thus, suppose that the rotation frequency of the frame is some constant μ. Then introduce a new variable for each oscillator:

$$\theta_i' = \theta_i - \mu t \Rightarrow \theta_i = \theta_i' + \mu t.$$

So $\dot{\theta} = \dot{\theta}_i' + \mu$. Substituting this into the original model:

$$\dot{\theta}_i' + \omega_i - \mu + \frac{K}{N}\sum_{j=1}^{N} \sin\left(\theta_j' + \mu t - (\theta_i' + \mu t)\right),$$

$$\Rightarrow \dot{\theta}_i' = (\omega_i - \mu) + \frac{K}{N}\sum_{j=1}^{N} \sin\left(\theta_j' - \theta_i'\right). \tag{5}$$

Eq. (5) is the governing equation in the rotating frame, but it is still a Kuramoto model. Since all frequencies have been shifted equally by their mean, the mean frequency has no change since $\mu - \mu = 0$. The term $(\omega_i - \mu)$ is, in fact, the **detuning** term for each oscillator with respect to the frame frequency [6]. Let $(\Omega_i = \omega_i - \mu)$, if Ω_i is positive, then the oscillator is running faster than others, whereas for negative values it is running slower. We shall define a new distribution for the detuning indicated by $G(\omega) = g(\mu + \omega)$. Since $g(\mu + \omega) = g(\mu - \omega)$ we see that $G(\omega) = G(-\omega)$, that $G(\omega)$ is an *even*, or equivalently, a symmetric function.

3 Steady state analysis in large populations

To see whether the synchronization may occur or not, we need to analyse the evolution of the order parameter. To do this, first we should consider a type of distribution for the system, which means to allow $G(\omega)$ to have infinite tails, and then try to figure out what the relation is between the order parameter and the coupling strength. We seek coupling strengths at which the transitions occur. Through this observation, it seems that there is a critical value for the coupling strength where $r(t)$ behaves differently. Denote this critical value by K_c. For values less than K_c, no specific coherence can be seen, and the phases of the oscillators are distributed uniformly around the circle. Once K exceeds the critical threshold value K_c, a phase transition occurs. This corresponds to the instability of the incoherent state of the system, where $r(t)$ demonstrates exponential growth. Through this phase transition, $r(t)$ saturates at some asymptotic values $r_\infty < 1$. Figure 3 illustrates this. Due to strict inequality, some oscillators mutually synchronize and eventually the whole population splits into two distinct clusters: the group of synchronized oscillators that are phase-locked and oscillate with frequencies close to the mean of the frequencies and co-oscillate with the average phase $\psi(t)$ [2]; a second group that rotate independently with frequencies at the tails of the distribution.[1] This situation is usually called *partial synchronization*. Let us explore this in more detail. We look for stationary points of an infinite-N Kuramoto model with nonzero coupling strength $(K \geq 0)$.

1 One reason for choosing distributions with finite tails is to prevent asynchronous oscillations as much as possible. This will be discussed later in this article.

As discussed above, we assume that in steady state the ordering parameter is constant and the system oscillates with the average phase $\psi(t)$ and the mean frequency μ, that is, $r(t) = r_\infty$ and $\psi(t) = \mu t$. This is the conjecture of Kuramoto's original analysis [3]. In the rotating frame, the phase equation changes to $\psi = \Psi - \mu(t)$. Kuramoto conjectured that the infinite-N model has a steady state for which the order parameter remains constant, and $\psi \equiv 0$ [3, 5]. By this assumption, we can reform the equation in a way that properly decouples each oscillator.

$$\dot{\theta}_i = \Omega_i - Kr_\infty \sin\theta_i.$$

Now consider the vector field of this equation $\Omega_i - Kr_\infty \sin\theta_i$, when $\Omega_i > 0$. We observe two stationary points, where the one closest to zero is stable. We have: $Kr \sin\theta_i^* = \Omega_i$. Oscillators with $|\Omega_i| \leq Kr$ are said to be **phase-locked**, once they have become stuck at their stable stationary point. This can be seen by the following simple analysis:

$$\Omega_i > 0 \rightarrow \dot{\theta}_i = \Omega_i - Kr \sin(\theta)_i = 0,$$

$$\Rightarrow \Omega_i = Kr \sin(\theta_i^*) > 0 \rightarrow \frac{\Omega_i}{Kr} = \sin\theta_i^*,$$

$$\Rightarrow \theta_i^* = \arcsin\frac{\Omega_i}{Kr} \rightarrow 0 < \theta_i^* < \frac{\pi}{2}.$$

By linearization of the equation about the steady point, we see the following:

$$\frac{\partial}{\partial\theta_i}(\Omega_i - Kr\sin\theta_i) = -Kr\cos\theta_i^* < 0.$$

Negativity ensures the stability of this steady state. So, the clustered oscillators remain in phase-locked status. However, remember that this is for the averaged system (rotating frame). In the original system, this is equivalent to phase-locked oscillators running around the circle as a cluster of oscillators. These synchronized oscillator phases span the right semicircle of the plane. Their speed is distributed uniformly, as the tranquil one is set at $\theta_i^* = \frac{-\pi}{2}$, and the speedy one is set at $\theta_i^* = \frac{+\pi}{2}$. This evidence reveals that oscillators with frequencies in the middle area ($|\Omega_i| \leq Kr$ are synchronized (stable)). When ($|\Omega_i| \leq Kr$), the graph of $\dot{\theta}_i$ crosses the θ_i- axis two times. Otherwise, when ($|\Omega_i| > Kr$), the vector field does not cross the θ_i-axis, so we do not have any points. Thus, there would not be any phase-lock incidence, and all oscillators rotate monotonically, but not uniformly! That is, at some points they all run slowly and at other points they run quickly. When ($|\Omega_i| > Kr$), in the original system, each oscillator tries to *drift* the phase-locked group ($|\Omega_i| \leq Kr$). Rapid ones take over and slower ones stay behind.

The contribution of the drifting oscillators

Assume infinitely many drifting oscillators in steady state, all having some particular frequency ω. These oscillators also obey the velocity rule $v(\theta, \omega) = \dot{\theta} = \omega - Kr\sin(\theta)$. At low speeds they are densely accumulated, whilst at high speeds they are thinly distributed [5]. This distribution is quite invariant because even if one of the oscillators gets out of the group, another one will take its place. Kuramoto [3] guessed that drifters in fact make a kind of distribution which is inversely

proportional to the velocity, specifically (see [3, 5]):

$$\rho(\theta,\omega) = \frac{C}{|\omega - Kr\sin\theta|}.$$

At $\theta = \frac{\pi}{2}$, drifters have their lowest speed, since for $\omega > Kr$, $v(\theta,\omega)$ is at the minimum value, while $\rho(\theta,\omega)$ has its highest value at this phase. To find C in $\rho(\theta,\omega)$, we note that $\rho(\theta,\omega)$ is a density function, so that

$$\int_0^{2\pi} \rho(\theta,\omega)d\theta = 1.$$

Then, $C = \frac{\sqrt{\omega^2 - K^2R^2}}{2\pi}$.

Self-consistency

To confirm that these ideas about the order parameter are consistent with the original form, we can average the population of all phase oscillators in the circle by $< e^{i\theta} >$. This can be split into two subpopulations, first the phase-locked oscillators and a second group of drifting oscillators. So,

$$< e^{i\theta} > = < e^{i\theta} >_{lock} + < e^{i\theta} >_{drift} .$$

Note that the average phase ψ here should be zero, so that $< e^{i\theta} > = re^{i\psi} = r$. Then we have the following.

$$\rightarrow r = < e^{i\theta} >_{lock} + < e^{i\theta} >_{drift} . \tag{6}$$

Here we can take into account the functional features of the probability distribution function $g(\omega)$ to calculate the explicit form of Eq. (6). Through the calculations, we can see that the integrals of the drifting oscillators will vanish due to the oddness of the integrands and Eq. (6) only depends on the phase-locked contributions. We avoid discussing further details of the calculations here, but they can be found in [5]. Finally, we catch up with the following equations:

$$r = Kr\int_{\frac{-\pi}{2}}^{\frac{\pi}{2}} \cos^2\theta g(Kr\sin\theta)d\theta,$$

$$\rightarrow r\left(1 - K\int_{\frac{-\pi}{2}}^{\frac{\pi}{2}} \cos^2\theta g(Kr\sin\theta)d\theta\right) = 0.$$

Obviously, we can observe that there is a trivial solution $r = 0$, which corresponds to the incoherent state [2]. The second set of solutions corresponds to partially synchronized oscillators that satisfy the following relation simply by removing r on both sides:

$$1 = K\int_{\frac{-\pi}{2}}^{\frac{\pi}{2}} \cos^2\theta g(Kr\sin\theta)d\theta.$$

Leaving $r \to 0^+$, we can easily find the critical coupling strength as follows:

$$1 = K \int_{\frac{-\pi}{2}}^{\frac{\pi}{2}} \cos^2\theta g(0) d\theta \Rightarrow K_c = \frac{1}{\pi g(0)}. \tag{7}$$

The key point within this process is that the partially synchronized states bifurcate at $K = K_c$. To unravel this bifurcation, we can approximate the integral (7) by expanding in terms of the powers of r [2]. This shows that the bifurcation is *supercritical* if $g''(0) < 0$ and *subcritical* of $g''(0) > 0$. Imposing the *square-root scaling law*, the amplitude of the partially synchronized oscillations is roughly equal to:

$$\sqrt{\frac{16}{\pi K_c^3}} \sqrt{\frac{K - K_c}{-K_c g''(0)}}.$$

The second square root represents the *normalized* distance above the threshold [2].

What does the critical coupling tell us?
The key concept is the role of $g(0)$. Recall that the density function is symmetric and unimodal. Additionally, for the rotating frame, the mean frequency is equal to zero, which is also the mode of distribution. So, g(0) is the highest number of frequencies in the PDF graph. In addition, it satisfies the normalization condition; therefore, it reveals that there is a box of the same height whose area should be equal to one. This means that the width of this box should be proportional to $\frac{1}{g(0)}$ to see the synchronization. $\frac{1}{g(0)}$ still works in the case of distributions with infinite tails and measures the width properly. So, based on these interpretations, we see that $K_c = \frac{2}{\pi g(0)}$ expresses the proportional relation of the critical coupling strength to the width of the frequency distribution. For any arbitrary distribution, it is possible to investigate the referred phenomena as Kuramoto did in his revolutionary articles [3, 4].

4 Reduction methods for the complexity

Ott-Antonsen ansatz

We focus on the Kuramoto model in the limit $N \to \infty$. Then, the state of the oscillator system at time t can be described by a continuous (with respect to frequency ω as well as phase θ) distribution function $f(\theta, \omega, t)$, where:

$$\int_0^{2\pi} f(\theta.\omega, t) d(\theta) = g(\omega). \tag{8}$$

In Eq. (8), $g(\omega)$ is the time-independent oscillator's frequency distribution function.
Consider Eq. (8). In their seminal work, Ott and Antonsen [7] show that:

i. Specific conditions satisfied by the initial distribution $f(\theta, \omega, 0)$ are maintained by $f(\theta, \omega, t)$;
ii. For an appropriately chosen frequency density $g(\omega)$, the macroscopic dynamics obeys a finite number of nonlinear ODEs.

The key purpose of (i.) is the invariance of the subspace of the state space, where the dynamics of the system remain. Ott and Antonsen [7] interpreted this in terms of the *existence of a manifold of space D of all possible distribution functions*. The manifold M should be invariant in the evolution of the system. For (ii.), we should refer again to the order parameter to clarify the macroscopic be-

haviour of the system. In fact, this parameter quantifies the global degree of coherent behaviour of oscillators in terms of integration of the distribution function in the domain of natural frequencies and the phase of oscillations [7]:

$$r = \int_0^{2\pi} \int_{-\infty}^{+\infty} f e^{i\theta} d\omega d\theta. \tag{9}$$

According to (ii.), the evolution of the order parameter is finite-dimensional even if the subspace (manifold) M and the function f, through its dynamics in M, are infinite-dimensional. Through this analysis, Ott and Antonsen proposed a much simpler method to investigate the dynamical behaviour of the system through an exact closed-form solution for the Kuramoto model [7, 8]. Assuming (i.) and (ii.), Ott and Antonsen [7, 8] proceeded as follows: First, the coupling in the Kuramoto model can be written as follows:

$$\frac{1}{N}\sum_{j=1}^{N} \sin(\theta_j - \theta_i) = Im\left(e^{-i\theta_i}\frac{1}{N}\sum_{j=1}^{N} e^{i\theta_j}\right) = Im(re^{-i\theta_i}).$$

With $N \to \infty$, the distribution function f should satisfy the **continuity equation**. In addition, oscillations flow through the phase space with velocity $v(\theta, t)$ determined by the coupling function and intrinsic dynamics. So, $f(\theta, \omega, t)$ satisfies the following partial differential equation:

$$\frac{\partial f}{\partial t} + \frac{\partial}{\partial \theta}(vf) = 0,$$

with $v(\theta, t) = \dot{\theta} = \omega + Kr\sin(\psi - \theta)$ or equivalently as $v(\theta, t) = \omega + \frac{K}{2i}(re^{-i\theta} - r^* e^{i\theta})$. So, the continuity equation accepts the following form [7]:

$$\frac{\partial f}{\partial t} + \frac{\partial}{\partial \theta}(vf) = \frac{\partial f}{\partial t} + \frac{\partial}{\partial \theta}\left(\left((\omega + \frac{K}{2i})(re^{-i\theta} - r^* e^{i\theta})\right)f\right) = 0, \tag{10}$$

where (r) is the same as in Eq. (9). The rate of change for $f(\theta, \omega, t)$ at a point in phase space $(\frac{\partial f}{\partial t})$ is balanced by the *inflow* and *outflow* of oscillators to that point $\frac{\partial}{\partial \theta}(vf)$. Since $f(\theta, \omega, t)$ is a 2π-periodic function, we can expand it as a *Fourier* series in phase [9]:

$$f(\theta, \omega, t) = \frac{1}{2\pi}\sum_{-\infty}^{\infty} f_n(t, \omega) e^{-in\theta},$$

where the n^{th} Fourier coefficient is:

$$f_n(t, \omega) = \int_0^{2\pi} e^{in\theta} f(\theta, \omega, t) d\theta, \quad n \in \mathbb{N},$$

or in complex form [7]:

$$f(\theta, \omega, t) = \frac{g(\omega)}{2\pi}\left[1 + \sum_{n=1}^{\infty} f_n(\omega, t) e^{in\theta} + c.c\right],$$

where $c.c$ denotes the *complex conjugate*, and the presence of $g(\omega)$ is the result of the relation

$$\int_0^{2\pi} f(\theta,\omega,t)d\theta = g(\omega).$$

Ott and Antonsen [7, 8] considered a restricted class of $f_n(\omega,t)$ such that:

$$f_n(\omega,t) = \alpha^n(\omega,t),$$

where $|\alpha(\omega,t)| \leq 1$, which prevents the divergence of the series. A remarkable result will be obtained by substituting this series expansion into Eq. (10) as:

$$\frac{\partial\alpha}{\partial t} + \frac{K}{2}(r\alpha^2 - r^*) + i\omega\alpha = 0, \tag{11}$$

$$r^* = \int_{-\infty}^{\infty} \alpha(\omega,t)g(\omega)d\omega. \tag{12}$$

As can be seen, this assumption transforms the phase-dependent equation into a θ-independent problem. Performing the summation of the Fourier series using the geometric series law gives [9]:

$$f(\theta,\omega,t) = \frac{g(\omega)}{2\pi}\frac{(1-|\alpha|)(1+|\alpha|)}{(1-|\alpha|^2)+4|\alpha|\sin^2(\frac{1}{2}(\theta-\psi))}.$$

Here, $\alpha \equiv |\alpha|e^{-i\psi}$ and ψ is a real quantity. For the values of $|\alpha| < 1$, it can be observed that the latter equation for $f(\theta,\omega,t)$, $f \geq 0$ [7], and its phase average is equal to $\frac{g(\omega)}{2\pi}$. In order to see that the set of Eqs. (11) and (12) represent a solution of Eq. (9) for any finite time, $\alpha(\omega,t)$ should evolve under the dynamics of Eqs. (11) and (12), together with the condition $|\alpha(\omega,t)| \leq 1$ to be continuously satisfied. Accordingly, we have the following form:

$$\frac{\partial|\alpha|}{\partial t} + \frac{K}{2}(|\alpha|^2-1)Re(re^{-i\psi}).$$

By substituting $\alpha = |\alpha|e^{-i\psi}$ and taking the real part after multiplying by e^{ψ}. At $|\alpha| = 1$, the second term of this new form vanished and we have $\frac{\partial|\alpha|}{\partial} = 0$. This is identical to the invariance of the unit circle under the evolution of the solution (trajectory) starting from the initial condition $|\alpha(\omega,0)| < 1$ for all finite times. Here, someone may ask a question about why Ott and Antonsen [7, 8] chose the powering form for the ansatz. The key reason that convinced them to assume this type for the ansatz is that both stationary states of the Kuramoto model, either the incoherent state or the partially synchronized state corresponding to ($f = \frac{g}{2\pi} \equiv \alpha = 0$) and $r = C > 0$, respectively, conform to $f_n = \alpha^n$. Thus, this ansatz connects both states by specifying a family of distribution functions. To proceed, another restriction on the assumed form of $f(\theta,\omega,t)$ should be imposed; it is necessary to complexify $\alpha(\omega,t)$ from the real plane to the complex plane while keeping it analytically continuable. This continuation should not have singularities in the lower half ω plane and control its tendency $|\alpha(\omega,t)| \to 0$ as $Im(\omega) \to -\infty$ [7, 9]. As we discussed before, if this condition is satisfied for the initial condition, then it would be right for all finite times later. This can be easily seen, if $\omega_i = Im(\omega)$ for large negative quantities, then the following equation says

$\alpha(\omega,t) \to 0$as $\omega_i \to -\infty$:

$$\frac{\partial \alpha}{\partial t} + \frac{K}{2}(r\alpha^2 - r^*) + i\omega\alpha \approx \frac{\partial \alpha}{\partial t} + |\omega| t = 0.$$

Further details on the stability analysis of Kuramoto solutions with this ansatz can be found in [7]. So, Ott and Antonsen [7, 8] provided a finite set of nonlinear differential equations that demonstrate the macroscopic evolution of the original system, and allows to study the dynamics of the oscillators in infinite-size but with reduced system. The next subsection discusses a recently introduced method for complexity reduction.

Recently developed method for complexity reduction in the 3D-Kuramoto model

As we saw, Ott and Antonsen [7, 8] provided us with an ansatz for the density function of the Kuramoto oscillators to derive a set of equations to reduce the dynamical complexity. In [10], a new method is proposed to construct an ansatz for a 3-dimensional Kuramoto model based on spherical harmonics for the density function. Although different from Ott and Antonsen [7, 8], the results are quite similar. The advantage of this new method is that it can be generalized to higher-dimensional systems. To explain the idea briefly, the set of equations is [10]:

$$\frac{d\vec{\sigma}_i}{dt} = W_i\vec{\sigma}_i + \frac{1}{N}\sum_j \left[K_i\vec{\sigma}_i - (\vec{\sigma}_i.K\vec{\sigma}_j)\vec{\sigma}_i\right].$$

Here $\vec{\sigma}_i$ is the rotation unit vector, W_i is a 3×3 antisymmetric frequency matrix, K_i is the 3×3 coupling matrix. In this modification, each oscillator has three independent frequency components that are sampled from a normalized distribution $G(\vec{\omega})$. The order parameter can also be defined as $\vec{r} = \frac{1}{N}\sum_i \vec{\sigma}_i$. Let $\vec{q}_i \equiv K_i\vec{r}$ and rename $\vec{\sigma}$ as $\hat{r}$. Then the evolution dynamics can be represented as

$$\dot{\hat{r}}_i = \vec{w}_i \times \hat{r}_i + \vec{q}_i - (\hat{r}_i.\vec{q}_i)\vec{r}_i.$$

This is invariant under any transformation of $\vec{q}_i \to \vec{q}_i + a_i\vec{r}_i$. Following this, the ansatz for the density function is:

$$f(\vec{\omega},\theta,\phi,t) = \frac{G(\vec{\omega}}{4\pi}\left[1 + 4\pi\sum_{l=1}^{\infty}\sum_{m=-l}^{l}\rho^l Y^*_{lm}(\theta,\Phi)Y_{lm}(\theta,\phi)\right].$$

Here, the continuity equation takes the form:

$$\frac{\partial f}{\partial t} - 2fq_r + (\omega_\phi + q_\theta)\frac{\partial f}{\partial \theta} + \frac{1}{\sin(\theta)}(-\omega_\theta + q_\phi)\frac{\partial f}{\partial \phi} = 0. \tag{13}$$

Eq. (13) is the result of considering $\vec{v} = \vec{\omega}\times\vec{r} + \vec{q} - (\vec{r}.\vec{q})\vec{r}$ and computing the partial derivatives in the spherical form of the continuity equation.

$$\frac{\partial f}{\partial t} + \frac{1}{\sin\theta}\frac{\partial}{\partial\theta}(f\sin\theta v_\theta) + \frac{1}{\sin\theta}\frac{\partial}{\partial\theta}(f v_\theta) = 0.$$

Further details of this analysis and the stages of the approach can be found in [10].

5 Extensions of the Kuramoto model

Stochastic Kuramoto model

Since the main purpose of this article concerns neuronal activity in the brain, it is worth discussing extensions of the Kuramoto model to encompass real-physical phenomena such as brain neuronal bursting. Since neurons interact with each other via biochemical transmissions, they always deal with noise effects. A major reason is that they are exposed to various kinds of noise, such as stochastic openings and closings of the ionic channel and subsequently some spontaneous neurotransmissions that trigger unpredicted depolarization and hyperpolarisation [11]. Another form of noise in neuronal activities is the result of external forces such as artificial electrical pulses, or effects of some chemicals like alcohol on brain's functions, where the brain has to process the noisy sensory information [12]. For example, temperature variations and hormonal fluctuations can affect the synchronization of the neurons within brain networks. Based on these observations, it makes sense to add noise terms in our theoretical analysis. In the case of synchronization models, noise may influence synchrony as an additive stochastic term. In the Kuramoto model, this can be represented as a perturbation term as below:

$$\dot{\theta}_i = \omega_i + \frac{K}{N}\sum_{j=1}^{N}\sin(\theta_j - \theta_i) + \xi_i(t),$$

where $\xi_i(t)$ captures the stochastic noise effect. This form of the Kuramoto model is known as *stochastic Kuramoto model*. Usually, $\xi_i(t)$ is *Gaussian white noise* so that [13]:

$$< \xi_i(t) >= 0, \quad < \xi_i(t)\xi_j(t) >= 2D\delta_{ij}\delta(t-t').$$

In [13] an explicit analysis of the stochastic Kuramoto model has been provided, where they have exploited a *Fokker-Planck equation* approach to reduce the system's dimension and so study the mean-field behaviour and onset of synchronization. The Fokker-Planck equation is a computationally efficient way of analysing stochastic differential equations. The Fokker-Planck approach can be used here to explore thermodynamic limits of the stochastic Kuramoto model. Indeed, the stochastic Kuramoto model can be reformed as follows [13]:

$$\dot{\theta}_i = \omega_i + rK\frac{k_i}{N}\sin(\psi - \theta_i) + \xi_i(t),$$

which is a representation in terms of mean-frequency, the order parameter and each each node's degree (k_i). This is equivalent to a Markov process with a transition probability $\mathcal{P}(\theta, t|\theta_0, t_0, \omega, k)$ where θ and θ_0 are N-vectors containing phases and likewise k and ω. This transition probability can be substituted in a Fokker-Planck equation:

$$\frac{\partial \mathcal{P}}{\partial t} = -\frac{\partial}{\partial \theta}(\mu\mathcal{P}) + \frac{\partial^2}{\partial \theta^2}(D\mathcal{P}),$$

yielding

$$\frac{\partial \mathcal{P}}{\partial t} = -\sum_{i=1}^{N}\frac{\partial}{\partial \theta_i}\left[(\omega_i\mathcal{P} + k_i\frac{K}{N}\sum_{j=1}^{N}\frac{k_j}{\sum_{m=1}^{N}K_m}\sin(\theta_j - \theta_i)\mathcal{P})\right] + D\sum_{i=1}^{N}\frac{\partial^2\mathcal{P}}{\partial \theta_i^2}.$$

The detailed analysis of the continuity equation for stochastic Kuramoto models can be found in [13]. For numerical simulations and further analysis of the stochastic Kuramoto model can be found in many papers, especially [14]. To conclude this part, we recommend the article [15] to see the impact of noise on synchronization and how noise actually increases the synchronization threshold. Here, the dependence of thresholds for, and levels of, synchronization on the strength of the noise and correlation times are explored.

Second-order Kuramoto model

Up to now, we have surveyed several types of the Kuramoto model in terms of first-order differential equations. The first-order Kuramoto model is favoured because of its tractability and capacity to model and represent a vast number of synchronization patterns. In [14], they found that a modified second-order Kuramoto model proceeds to synchronization much faster than the realistic phenomena. To overcome this bug, it is necessary to apply infinite coupling strength to achieve perfect synchrony [13]. One key assumption in the original Kuramoto model is that instantaneous adjustment of their frequencies in response to interactions. But this is quite far from the realistic nature of oscillatory networks. As an example, in case of neuronal activities, neurons can not instantaneously adjust their firing rate. The other inefficiency of the first-order Kuramoto model is the absence of *inertia* which means it does not include the resistance of coupled oscillators in their frequency changes until reaching a synchronized level.
In 1991, Ermentrout proposed a model with adaptive frequencies that is able to represent the synchrony between oscillators. This allows both phase and frequency to evolve in time and the inertia rebates the synchronization dynamics [16]. Adding this inertia term smooths the instantaneous variations and considers short-time oscillations more accurately, and enables us to investigate more complex dynamics such as transient and quasiperiodic behaviours. In the context of neural oscillations, we should consider that neuronal activities have temporal memory(*hysteresis)* where the system's state depends on its previous activities. First-order Kuramoto model does not include this feature due to the lack of inertia. Additionally, in case of neural disorders like the Parkinson's disease and epilepsy, there are strong complex dynamical variants which can not be described by the first-order Kuramoto model. In contrast, second-order Kuramoto model can perfectly reveal the dynamics of these disorders. For instance, in Parkinson's disease, brain oscillators undergo overshooting synchronizations. While the first-order Kuramoto model typically shows monotonic evolution toward synchronization, the second-order Kuramoto model allows the overshooting phenomena to take place naturally. Finally, let's see what is a second-order Kuramoto model. The governing equation is [13]:

$$\ddot{\theta}_i + \alpha\dot{\theta}_i = \omega_i + K\sum \mathcal{A}_{ij}\sin(\theta_j - \theta_i), \tag{14}$$

where α is the *dissipation parameter*. By setting $\ddot{\theta}_i = 0$ in Eq. (14), we get back to the original Kuramoto model. Another capability of this new second-order form is the exhibition of a *bistability* region where oscillators move between synchronous and asynchronous states [13]. The $\dot{\theta}_i$ acts as a *damping* term that represents the *ith* node resistance again change of frequency. Without such a term the indefinite oscillations are feasible. In [13], the single neuron equation within an infinite-N size grid has been considered as:

$$\ddot{\theta} = -\alpha\dot{\theta} + \omega_K \sin(\theta_L - \theta),$$

where θ_L is the phase of the large system, without a loss of generality let's set $\theta_L \equiv 0$.

By defining the energy function $E(\nu, \omega) = E_k(\nu) + E_P(\theta)$ where ν is the *angular speed* and the right hand side terms can be obtained as $E_k(\nu) = \frac{\nu^2}{2}$ as the *kinetic energy* and $E_P(\theta) = -\omega\theta - K\cos(\theta)$ as the *phase energy*. These can be easily calculated by the energy integral. In the absence of damping term and zero frequency $(\alpha = 0, \omega = 0)$ and defining a dimensionless time variable $\tau = \sqrt{Kt}$, this equation transforms into:

$$\frac{d^2\theta}{d\tau^2} = -\sin(\theta).$$

The bifurcation analysis of this equation has been done in [13] where it has two fixed-points $(\pi, 0)$ and $(0, 0)$ that are *saddle* and *centre* nodes respectively. For small values of damping and starting from $\omega > 1$, the system oscillates periodically. By slowly decreasing the frequency down to some critical value $\omega_c < 1$ rotations merge with the saddle and annihilate in a homoclinic bifurcation. As damping tends to zero, the bifurcation border splits the regions of bistability and globally stable fixed point. Further details of bifurcation analysis and mean-field analysis can be found in [13] and [16]. Another interesting configuration of second-order Kuramoto model is the emergence of some extra stochastic noise term. This modification has been shown in [14]:

$$\ddot{\theta} = -\alpha\dot{\theta} + \omega_i + K\sum_{j=1}^{N} \mathcal{A}_{ij}\sin(\theta_j - \theta_i) + \xi_i(t),$$

or equivalently:

$$\ddot{\theta}_i = -\alpha\dot{\theta}_i + \Omega_i Kr\sin(\psi - \theta_i) + \xi_i(t),$$

where again similar to the previous analysis of the stochastic Kuramoto model using the Fokker-Planck equation as a perfect stochastic analysis technique is essential. In [14] a comprehensive discussion around the various features, modifications and analysis has been provided, specifically a nonlinear Fokker-Planck equation analysis for the stochastic resonance phenomenon within the second-order Kuramoto model.

Applied variants of the Kuramoto model

In this sub-section, we briefly review variations of the Kuramoto model that find applications in modelling of natural oscillations such as neural oscillations. One example, introduced first by *Sakagushi* [17], is the original Kuramoto model with an extra external force:

$$\dot{\theta}_i = \omega_i + \frac{K}{N}\sum_{j=1}^{N}\sin(\theta_j - \theta_i) + \Lambda\sin(\Omega t - \theta_i).$$

This form models mammalian circadian rhythms in the brain where oscillatory neurons are stimulated by variations of sunlight. Λ represents the amplitude of the sinusoidal force and Ω is the mean frequency of the oscillatory population [7].

A second variation is the so-called multi-population Kuramoto model. This model captures oscillators belonging to specific cohorts or, better to say, communities. It allows us to study inter-cluster and intra-cluster synchronization patterns and also investigate the level of impact

that each community has on others. A general form of this type is [7, 18]:

$$\dot{\theta}_i^\sigma = \omega_i^\sigma + \sum_{\sigma'=1}^{s} \frac{K_{\sigma\sigma'}}{N_{\sigma'}} \sum_{j=1}^{N_{\sigma'}} \sin(\theta_j^{\sigma'} - \theta_i^\sigma), \quad i = 1, \ldots, N_\sigma, \quad \sigma = 1, \ldots, s.$$

Here, N_σ is the size of the population of the type σ, and $K_{\sigma\sigma'}$ is the coupling strength between oscillators in cluster σ' and oscillators in cluster σ. This model was analyzed through both the stability and numerical analysis of solutions in [18]. An intriguing application of this multi-population model is to simulate excitatory-inhibitory activities of neurons and their influence on brain activities. This will be discussed in the next section of the paper.

6 Kuramoto model in neural networks

How do neurons speak to each other?

Neural communications basically take place via two types of biological signals, electrical and chemical. These electrical messages are driven by ions within the neuron from one end of the nerve cell to the other side. Inter-neuronal communications occur at *synapses*, where presynaptic and postsynaptic neurons get close to each other to transmit the chemical substances. This dialogue starts when presynaptic neurons release a neurotransmitter which is a chemical matter and the postsynaptic neurons receive it via their specialized protein called *neurotransmitter receptor*. This neurotransmitter binds to the receptor protein and changes postsynaptic neuron's activity. There are two types of neurotransmitter receptors [12]:

- *ligand-gated ion channels*(LGIC): this type allows rapid ionic flows to across the membrane of the neuron directly;
- *G-protein-coupled receptor*(GPCR): This type sets into the motion of chemical message inside the neuron

Neurons are distinguished from other cells of the body by having specific tiny branches called *dendrites* and *axons*. Dendrites are responsible for receiving chemical inputs from other neurons, with information exchanges achieved through through axons. The membrane of neurons contains plenty of ion channels where ion particles pass through them during opening and closing of ion-gates. One significant implication of this voltage-gated channel is production of rapid signals, known as *action potential* [11, 12], which is the quickest mode of intracellular communications in neural networks. Synaptic responses are mainly settled by LGIC to create *excitatory-inhibitory* activities [12]. Activation of these kinds of receptors usually triggers an influx of Sodium ion into the nerve cell and results in the membrane potential to depolarizing (positive ionic degree), pushing the neuron closer to action potential threshold. Regarding the inhibitory synaptic transmissions, receptors in ionic channels permit the negative ions to flow and when they are fully activated, they allow the hyperpolarisation of membrane potential take place. On the other hand, slower but longer responses are mediated by GPCR due to several extra molecular steps needed to get from receptors to effectors. They are much slower compared to LGIC proteins because they usually activate ionic flows indirectly [12]. Thus, the type of synaptic transmissions enabled by GPCR are called *neuromodulatory*. We have reviewed briefly what happens when neurons communicate with each other. A fundamental neuronal activity, and the foundation of neural interactions, is *excitatory-inhibitory regime* taking place within networks of neural populations. This activity has a synchronization nature where two types of neurons with different behaviour interact and affect each other. Due to its synchronous nature, this phenomenon can be modelled via the Kuramoto model. This is considered in the next section.

Kuramoto model in excitatory-inhibitory neural behaviours

In excitatory-inhibitory neuronal rhythms, two groups of oscillating neurons interact with each other. Here one group of neurons are the fast-acting excitatory neurons, the other group is the slow-acting inhibitory neurons. These two groups interact with each other via pulse-coupling communications according to Winfree's model [1]:

$$\dot{\theta}_i^\sigma = \omega_i^\sigma + \xi_i^\sigma + Q(\theta_i^\sigma)(K_{\sigma E}h_E - K_{\sigma I}h - I),$$

with the Lorentzian distribution of $(\gamma, \overline{\omega}_\sigma)$:

$$g_\sigma(\omega) = \left(\frac{\gamma}{\pi}\right)\left[(\omega - \overline{\omega}_\sigma)^2 + \gamma^2\right]^{-1},$$

where ξ_i^σ is the zero-mean delta-correlated noise term of strength $D :< \xi_i^\sigma(t), \xi_i^{\sigma'}(t) >= 2D\delta(t - t')\delta_{ij}\delta_{\sigma,\sigma'}$, and Q is the *phase response curve* that represents each oscillator's response to perturbations which are assumed to be $Q(\theta) = 1 - \cos(\theta)$, which is non-negative and thus results in phase advances or delays in response to excitatory-inhibitory inputs [19]. Neuronal oscillators with such kinds of phase response curve are called *type-1* [20]. Here h_E and h_I represent the mean-fields of excitatory and inhibitory neurons respectively and can be defined as:

$$h_\sigma = \frac{1}{N}\sum_{j=1}^{N} P(\theta_j^\sigma),$$

where $P(\theta_i^\sigma)$ is the produced-pulses of oscillators that should satisfy the integral $\int_{-\pi}^{\pi} P(\theta)d\theta = 2\pi$. In this excitatory-inhibitory regime each excitatory node exerts a positive pulse $P(\theta_j^E)$ with strength $\frac{K_{EE}}{N} \geq 0$ on the excitatory oscillators and with $\frac{K_{IE}}{N} \geq 0$ on the inhibitory oscillators. As described in [19], the excitatory-inhibitory oscillations start with a synchronous firing of excitatory neurons followed in response, by a synchronous firing of inhibitory neurons as a response. Here the excitatory activity can be considered as *fast dynamics* and inhibitory activities as *slow dynamics*. Now, by assuming that inter-regional activities are negligible and consider mean-frequency difference $\Delta\omega \equiv \overline{\omega}_E - \overline{\omega}_I > 0$. It is possible to shape the Kuramoto type model from the Winfree [19]:

$$\dot{\theta}_i^\sigma = \tilde{\omega}_i^\sigma + \xi_i^\sigma - \frac{1+r}{2N}\sum_{j=1}^{N}\left[K_{\sigma E}\cos(\theta_i^\sigma - \theta_j^E) - K_{\sigma I}\cos(\theta_i^\sigma - \theta_j^\sigma)\right], \tag{15}$$

where $\tilde{\omega}_i^\sigma \equiv \omega_i^\sigma + K_{\sigma E} - K_{\sigma I}$. This is a significant difference between this excitatory-inhibitory Kuramoto model and the original form. The natural frequencies of both the excitatory and inhibitory oscillators are shifted by the excitatory and inhibitory couplings strengths which, in turn, affect parameter-regions where this excitatory-inhibitory regime takes place. The other noticeable difference is the use of a cosine-type coupling instead of the original sinusoidal type. In [19] it has been shown that for some specific parameter values, if, at an initial time $t = 0$ the amplitude of the order parameters R_E and R_I, respectively for each excitatory and inhibitory cluster, are chosen to be zero, then similar to the original Kuramoto model, after a brief time, they both converge to some rotating solution $Z_\sigma(t) = R_* e^{i\psi(t)}$, where $0 < R_* < 1$ and $\dot{\psi}_\sigma = \Omega$ for $\sigma \in \{E, I\}$. This convergence is the onset of synchronization. Numerical simulations in [19] show

that the excitatory neurons precede the inhibitory neurons that is consistent with the previous assumptions of excitatory-inhibitory regime dynamics. Here the parameter (r) in Eq. (15) controls the strength of the neural pulse between clusters. By setting $(r = 1)$ we can reduce the width of pulses to be infinitesimally narrow similar to a Dirac delta pulses. This assumption simplifies the analysis of the model.

Analysis of an excitatory-inhibitory Kuramoto model

The Eq. (15) can be similarly analysed within the framework of a thermodynamics limit and letting $N \to \infty$. This would transform the set of phases and frequencies from pulse-like discrete data, into some continuous forms as $\{\theta_\sigma, \omega_\sigma\}$, for $\sigma \in \{E, I\}$. Subsequently, the density function also changes to the form $f^\sigma(\omega_\sigma, \theta_\sigma, t)$ [19]. Again, this density function should satisfy the continuity equation, or as we have already seen, the Fokker-Planck equation:

$$\frac{\partial f^\sigma}{\partial t} = -\frac{\partial}{\partial \theta_\sigma}(f^\sigma v_\sigma) + D\frac{\partial^2}{\partial \theta_\sigma^2} f^\sigma, \tag{16}$$

where we have $f^\sigma = \frac{1}{2\pi}$ for the completely incoherent state. Here again, because the f^σ functions are 2π-periodic, it is possible to use Fourier expansions and then substitute the Fourier expansion and the resulting Kuramoto order parameter in the continuity equation:

$$f^\sigma(\theta, \omega, t) = \frac{1}{2\pi}\sum_{l=-\infty}^{\infty} f_l^\sigma(\omega, t) e^{il\theta},$$

$$Z_\sigma = \left(\int_{-\infty}^{\infty} f_l^\sigma(\omega, t) g_\sigma(\omega) d\omega\right),$$

$$\xrightarrow{(16)} \frac{\partial}{\partial t} f_l^\sigma = -(il\tilde{\omega}_\sigma + lD^2) f_l^\sigma + \frac{il}{2} f_{l-1}^\sigma (K_{\sigma E} Z_E^* - K_{\sigma I} Z_I^*) + \frac{il}{2} f_{l+1}^\sigma (K_{\sigma E} Z_E - K_{\sigma I} Z_I). \tag{17}$$

Here $\tilde{\omega}_\sigma \equiv \omega_\sigma + K_{\sigma E} - K_{\sigma I}$. Then by using linearisation techniques for Eq. (17), we can investigate the stability of the incoherent solution. For sake of simplicity, it is helpful to consider all coupling strengths as the same, both the cross-couplings and self-couplings:

$$K_{EI} = K_{IE} \equiv K \;\; \& \;\; K_{II} = K_{EE} \equiv \epsilon K,$$

where $\epsilon \geq 0$ is the measuring parameter for the ratio of cross-and-self- couplings. After linearisation, the eigenvalues of the system are determined as [19]:

$$\lambda_\pm = -(\gamma + D) \pm \frac{\sqrt{K^2 - [\Delta\omega + (\epsilon - 2)K]^2}}{2} - i\Omega,$$

where $\Omega = \frac{\overline{\omega}_E - \overline{\omega}_I}{2}$ is the centre of natural frequency distribution of the population, including both excitatory and inhibitory neurons [19]. To find the critical limit of K, first, it should be denoted that the boundary of incoherence should be identified from the eigenvalue equation. To achieve this aim, in [19] they considered that γ and D have the same role here and by imposing $Re(\lambda_r) = 0$ (unstable situation for incoherence) we reach the following equation for the (critical) boundary of

synchronization:

$$\left(\frac{\Delta\omega}{\gamma+D}\right)_c^{\pm} = (2-\epsilon)\frac{K}{\gamma+D} \pm \sqrt{\left(\frac{K}{\gamma+D}\right)^2 - 4}. \tag{18}$$

A necessary condition for Eq. (18) to have real values is

$$\frac{K}{\gamma+D} \geq 2.$$

which is not a sufficient condition for synchronization but represents the critical value of coupling strength. Although the control parameter ϵ does not appear here, and the synchronization seems to only depend on K, however, ϵ controls the variations of frequency difference of two populations for stability of incoherence state. Indeed, if $\epsilon \leq 1$, then the boundary in Eq. (18) lies on the region where we have positive values for $\Delta\omega$. Thus, when $\Delta\omega < 0$, inhibitory neurons are faster than excitatory neurons, and we meet the stable incoherent state. By increasing ϵ, synchronous oscillators in excitatory-inhibitory networks emerge as inter-inhibitory neurons slow down, whereas excitatory neurons accelerate [11, 19]. So within this excitatory-inhibitory regime for the Kuramoto model we see that become established when excitatory neurons are ahead of inhibitory neurons and synchronization takes place when both groups cooperate. In case of faster inhibitory activities, synchronization is only possible for sufficiently large ϵ values.

Controlling the balance of excitatory-inhibitory activities

Maintaining a balance between excitiation and inhibition in the excitatory-inhibitory regime is cruical to so as to control the overall collective neuronal oscillations. This can be achieved by adding a sinusoidal interaction function, where excitatory neurons exhibit only attractive dynamics and inhibitory neurons exhibit only repulsive dynamics. This leads to categorizing the coupling strengths into four possible types: *intra-excitatory attractive activities* K_{EE}, *inter-inhibitory repulsive activities* K_{II}, *attractive interaction of excitatory neurons over inhibitory neurons* K_{EI}, and *the repulsive interaction of inhibitory neurons on excitatory neurons* K_{IE}. According there are then four types of Kuramoto model [21]:

$$\begin{cases} \dot{\theta}_{j,exc} = \omega_{j,exc} + K_{EE}R_{exc}\sin(\psi_{exc} - \theta_{j,exc}) - K_{IE}R_{inh}\sin(\psi_{inh} - \theta_{j,exc}), \\ \dot{\theta}_{j,inh} = \omega_{j,inh} + K_{EI}R_{exc}\sin(\psi_{exc} - \theta_{j,inh}) - K_{II}R_{inh}\sin(\psi_{inh} - \theta_{j,inh}), \end{cases}$$

where plus $(+)$ represents the *attractive* interaction and the minus $(-)$ represents the *repulsive* interaction. R_{exc} and R_{inh} are the order parameters of the excitatory and inhibitory neurons defined similarly by [21]:

$$R_\sigma e^{i\psi_\sigma} = \frac{1}{N_\sigma}\sum_{j=1}^{N_\sigma} e^{i\theta_{j,\sigma}}, \quad \sigma \in \{exc, inh\}.$$

To neutralize the rotating frame's frequency effect, the means of natural frequencies $\overline{\omega}_{exc} = \overline{\omega}_{inh} = \overline{\omega} = 0$. In [21], they have considered the density of excitatory and inhibitory neurons the same as fr the cortical and hippocampal neurons as $N_{exc} = 80\%$ and $N_{inh} = 20\%$. The frequency distribution of oscillators is considered to be Gaussian with zero mean and width=0.01. Then the total interaction strength for both excitatory and inhibitory neurons should be determined. These

interaction strengths $F_{exc}(t,\theta)$ and $F_{inh}(t,\theta)$ are extracted from the Kuramoto model equations for each group while assuming $\psi_{exc} \approx \psi_{inh} \approx \psi$ and oddness of sine function [21]:

$$\begin{cases} F_{exc}(t,\theta) = -K_{EE}R_{exc}\sin(\theta-\psi) + K_{IE}R_{inh}\sin(\theta-\psi), \\ F_{inh}(t,\theta) = -K_{EI}R_{exc}\sin(\theta-\psi) + K_{II}R_{inh}\sin(\theta-\psi). \end{cases}$$

These functions (F_σ) are attractive toward the resulting phase when $F(\theta-\psi)=0$ and $\frac{\partial}{\partial\theta}F<0$. Otherwise they are repulsive [5, 22]. Now, the collective dynamics can be studied via assessing the order parameter R of the system. Consequently, three types of dynamic states can be observed including, *synchronized*(high R), *bistable* (fluctuating R), and *asynchronous* (low R). The attraction of excitatory neurons on both themselves and the inhibitory neurons toward the same phase results to alignment of all mean-phases as $\psi_{exc} \approx \psi_{inh} \approx \psi$. The accumulation of excitatory neurons at the same phase triggers the bistable-cycle. This is due to mentioned reason that excitatory neurons attract all nodes of the system toward the same phase and the gathering of inhibitory neurons at the same phase ψ triggers the repulsive response over time, and leading to the stronger repulsive force than attractive force, resulting a considerable shift in interaction type [21].

However, this cutback in attractive force of excitatory neurons, leads to a dispersion of inhibitory neurons. This is the general bistability regime between excitatory and inhibitory neurons. During the time that K_{EE} is strong enough, the repulsive force of inhibitory neurons fails to overcome the attractive impact of excitatory neurons. This domination continues to accumulate all oscillators to achieve a synchronized state. On the other hand, while K_{II} is dominant, the mutual repulsion among inhibitory neurons decreases. When inter-group repulsion constants K_{EI} and K_{IE} are weak, the effect of repulsion from inhibitory neurons to excitatory neurons reduces and only synchronous behaviour can be observed among the excitatory neurons. Meanwhile, the inhibitory neurons demonstrate asynchronous behaviour [21]. In next topic, we will discuss an specific synchronization phenomenon within this excitatory-inhibitory environment.

Extreme synchronization events

A common phenomenon within brain neuronal activities is *excessive synchronization*. This indicates various pathologies and often the onset of neural disorders. Such undesired synchronization-related disorders can be understood using theoretical approaches. One thing that should be considered in brain studies which is usually ignored in theoretical models is the limitation on resources, available for neurons to synchronize. Hence, it is worth to introduce a new generation of the Kuramoto model considering this resource constrains.

In [23], it has been shown that there is a relation between increased excitability and the *explosive synchronization* caused by sequential network activities that pushes the system to demonstrate extreme synchronizations known as epileptic brain activities. As we discussed before, the excitations are due to the neurotransmitters which are transported as long as ion channels are active. Thus, the importance of resource consumption is reflected as a concerning topic. [23] provides us with a model of collective behaviour under excitability and resource constraints and has shown that the model exhibits extreme behaviour under the reciprocity of explosive synchronization and an increased excitability resource, as well as a sudden transition to synchronization while reducing the resource and finally end of synchronization. To achieve this aim, they have proposed a Kuramoto model via considering consumption constraints. This model will help us to survey extreme neuronal behaviours which is an important basis of many brain neural disorders in particular the epileptic activities. Once again, consider the original Kuramoto model as the following

form:

$$\dot{\theta}_i = \omega_i + K \sum_{j=1}^{N} \mathcal{A}_{ij} \sin(\theta_j - \theta_i),$$

where here $\mathcal{A}_{ij}$ is the connection matrix indicating whether there is an edge between the nodes (i) and (j) and K is the coupling strength. As a new approach, we shall divide the collective behaviours into *local* and *global* scales, reflecting the level of coherence in any region and globally as a whole. To accomplish this, [23] has proposed to define a *local order parameter* $r_i = \frac{1}{k_i} |\sum_{j=1}^{N} \mathcal{A}_{ij} e^{\theta_j}|$ where $k_i = \sum_{j=1}^{N} \mathcal{A}_{ij}$ is the degree of the i^{th} node. Global order parameter can also be defined as $R = \frac{1}{N} |\sum_{j=1}^{N} e^{\theta_j}|$. Another novel assumption is to consider natural frequencies depend on the degree of each node, equivalently as $\omega_i = k_i$. This idea is quite essential for exploring any potential explosive transitions in distinctive architectures. But as it can be seen, all of this material are somehow spontaneous variables and there is no any special control on them. The only parameter that can be varied and is under control is the coupling strength. Hence, K can be interpreted as excitability of neurons [23]. On the other hand, due to the resource constraints, this excitability does not long for prolonged time intervals. To overcome this issue, it is worth to consider the excitability (coupling) term as a time dependent function, together with being a function of local order parameter. Thus, the Kuramoto model will be transformed to the following system:

$$\begin{cases} \dot{\theta}_i(t) = \omega_i + K_i(t) \sum_{j=1}^{N} \mathcal{A}_{ij} \sin\big(\theta_j(t) - \theta_i(t)\big), \\ \dot{K}_i(t) = \alpha(K_i(t) - K_0) - \beta r_i(t), \end{cases}$$

where α is the *rate of excitability* recovery, and β is the resource limitation rate [23]. K_0 is the idealized excitability level in the absence of resource constraints (when $\beta = 0$). The so-called extreme behaviour in neuronal activities following the latter Kuramoto model, is possible via accosting of resource consumptions and explosive transitions. In [23], simulations of the model explore the macroscopic and microscopic behaviours of the system using several distinctive topological patterns and scales. This approach reveals, similar to excitation-inhibition, that there are three regions corresponding to synchronized, desynchronized and bistable states. Competition between explosive transitions and coherent state, and resource limitations and incoherent states, leads to short-time global coherence. This model provides a framework for studying abnormal or undesired synchronous or asynchronous phenomena in neuronal activities and links Kuramoto modelling to neural disorders, such as epilepsy and the Parkinson's disease. These issues are discussed in Section 7.

Architecture and the Kuramoto variations

There are some obvious similarities neuronal properties and those Kuramoto models. For example, the natural frequencies in the Kuramoto model can be interpreted as the firing rate of neurons. But there are some distinctions too. Indeed, in the original Kuramoto model the coupling strength K is the same for all nodes and the corresponding critical coupling strength is a constant value. However, each neuron behaves differently, for example, the coupling strength or firing rate depend on distance between neurons. A generalized Kuramoto model is considered in [24] where couplings are time-varying and specific for each pair of nodes. This leads to the constant coupling K being replaced by matrix of coupling strengths or, equivalently, a graph with weighted edges

describing a network of coupled neurons:

$$\dot{\theta}_i(t) = \omega_i + \frac{1}{N}\sum_{j=1}^{N} K_{ij}(t)\sin(\theta_j - \theta_i) \quad i = 1, 2, ..., N.$$

In brain neural networks, neurons are connected in various number of possible connection patterns. There are different scales to study the neuronal activities based on the network pattern. One is the macroscopic and the other is microscopic [25]. This makes difference in the interpretations and definition of mathematical objects in the graph of networks. For instance, to study these relationships, nodes and edges are defined distinctively. Based on the scale, nodes might be a single neuron or a cortical hub, and the edge between node can be whether a synaptic connection or an axonal fibre [25]. Back to the graph theory, two types of directions are common in networks of such model:

i. *unidirectional*
ii. *bidirectional*

In [24], five different types of connection topologies for small lattice of oscillators were incorporated to the Kuramoto model via their graph adjacency matrices as the coupling pattern $K_{ij}(t)$ and a new generalisation of the Kuramoto model was proposed as:
The five connection patterns are:

- *linear unidirectional*
- *linear bidirectional*
- *box unidirectional*
- *box bidirectional*
- *all-to-all*

where the last one is the original assumption of the Kuramoto model [3]. The graph of each arrangement has been shown in Figure 4. Through the examination of each arrangement via several constant coupling strengths, both *linear unidirectional* and *linear bidirectional* arrangements demonstrated the lowest level of coherence while increasing K except some instants of slight synchrony for bidirectional mode. In box arrangements, it can be seen that some strong synchronizations take place only on higher levels of couplings. *All-to-all* coupling represents the strongest synchronization patterns due to the full connections [24]. In spite of the significance of architecture patterns in level of synchronization, the couplings constant plays a crucial role in synchronization. This is observed when gradually increasing K and exceeding the threshold level, synchrony appears more and more [24]. Caution! unbounded increase of K may adversely affect and reverse the direction of synchronization.In fact, the correspondence between the definition of coupling constant in the Kuramoto model and its interpretation in neural networks is established by the sign of K. Positive sign means increasing coupling strength in terms of excitating synaptic activities, and consequently raising the level of neuronal synchrony, while the negative sign corresponds to inhibition in synaptic activities as discussed in the previous topic [24].Further details and analysis about *time-varying* K, various distribution effects on coupling strength, natural frequencies and the combination of assumptions for both of these parameters can be found in [24], [25].

Clustering, Coherence and Incoherence

Graph theory tools can be used to assess the complexity of networks such as neural networks. Two key graph theory indeces are the *average path length* (L) and the *clustering coefficient* (C) [25].

The path in a graph (or neural network) is a collection of edges (connections) between pairs of nodes. The path length or distance between nodes is related to transportation of chemical and electrical signals. There may be many paths between nodes so it makes sense to speak of average path length. Each node i in a network has a clustering coefficient C_i, obtained as follows. Firstly, each node in a graph defines a subgraph N_i of neighbours. The clustering coefficient C_i is the ratio of the number of connections the node i has to its neighbours to the number of connections N_i would have if totally connected. The clustering coefficient of the graph is then the mean of these clustering coefficients C_i. In an all-to-all coupled network $C = 1$.

This clustering coefficient can be incorporated in the Kuramoto model to study *local synchronization modes* through intra synchronous oscillatory clumps. In [26] it was shown that local synchronizations take place independently regardless of the connective patterns or the network topology. The synchronization modes in neural networks can be interpreted as a special kind of clustering problem. Basically the clustering problem aims to identify distinctive subsets of a population that share a common feature such as a collective behaviour or a structural pattern. Here the clustering is summarized to the local synchronization within a neural network. Let's employ this idea to the neural problem for a population of $N-$nodes regardless of the role of natural frequencies to increase the accuracy and only concentrate on connection patterns. Instead, for the global scale, [26] have proposed to consider some neighbourhoods for nodes to split the whole network into small ensembles of the populations N_i with the neighbourhood of the radius ϵ:

$$\dot{\theta}_i = \frac{K}{N_i} \sum_{j \in N_i} \sin(\theta_j - \theta_i).$$

To provide some index for the level of synchronization, we shall define an indicator denoted by r_c to indicate the termination of synchronization process. This can be defined as [26]:

$$r_c = \left| \sum_{i=1}^{N} \frac{1}{N_i} \sum_{j \in N_i} e^{\theta_j - \theta_i} \right|.$$

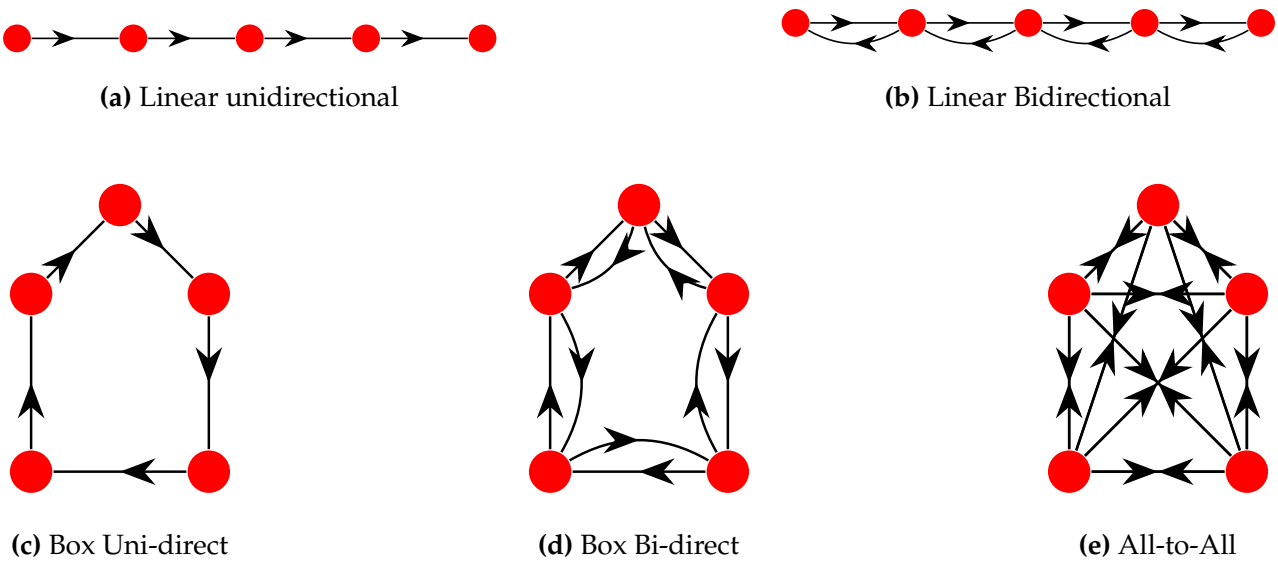

(a) Linear unidirectional

(b) Linear Bidirectional

(c) Box Uni-direct

(d) Box Bi-direct

(e) All-to-All

Figure 4. Five different topologies for a network of five nodes

This is a modified form of the order parameter in terms of cluster's synchronizations. But how the synchrony can spread out from local clusters to the whole network? in [26] a hierarchical approach was proposed. First, by defining appropriate coupling radius (distance) we observe the local clusters (equivalently $r \to 1$), the coupling radius of intra-cluster synchronizations increases. This can be interpreted as zooming out to one higher level. At this stage, the global synchronization takes place while the system order parameter tends to higher values near 1.

Clustering synchronization in networks of Kuramoto oscillators

Another perspective to study clustering equations in neural populations via the mighty Kuramoto model is to view the nonlinear dynamic aspects of oscillators. Similar to the past, the aim is to focus on networks that local synchronization (clustering) may take place. This happens when a subgroup of oscillators are coupled stronger with each other compared to their connections with the rest of the nodes. Additionally, they oscillate more synchronously with each other than with others. Here we just review another notion of the Kuramoto model for cluster-synchronization. In [27] they have analysed this problem via imposing some upper boundary to phase difference instead of considering the same equal phase for clustered oscillators. This allows to study cluster synchronization in any arbitrary topology, parameter variations and over asymmetric networks. Within this framework, again the Kuramoto network is considered as a connected, unidirected and weighted graph with the adjacency matrix (connection) $\mathcal{A}_{ij} = [a_{ij}]$, whose elements satisfy $a_{ij} \in \mathbb{R}_{\geq 0}$ (not necessarily binary inputs). The phase differences are also defined as a *geodesic* distance on the unit circle $\mathbb{S}^1$ as the Euclidean distance $|\theta_j - \theta_i|$. The Kuramoto model here is the same as before, where the natural frequencies are nonnegative real values. In [27] the definition of a cluster in this network has been provided as a subset of the nodes of the graph where a boundary $0 \leq \gamma \leq \frac{\pi}{2}$ exists such that if the initial phase difference satisfies it, then for any other times it still satisfies. In fact, they have shown that cluster interconnections are due to the strong intra-cluster couplings. In fact they have shown that cluster interactions are due to the strong intra-cluster couplings are comparably weaker than the inter-cluster connections. This culminates the harmony of natural frequencies (firing rates of neurons) within each cluster compared to the adjacent cluster [27]. Following this distinctive definition, they proposed a special indicator for clusterings. Briefly, let $\mathcal{C}$ be a subset of nodes within the network. Define:

$$\alpha_{max} = \max_{i,j \in \mathcal{C}} \left(\frac{(\omega_j - \omega_i) + \sum_{k \in \mathcal{C}} (a_{jk} + a_{ik})}{2a_{ij} + \sum_{k \in \mathcal{C}} \min(a_{ik}, a_{jk})} \right).$$

If $\alpha_{max} \leq 1$, then $\mathcal{C}$ is a synchronized cluster with respect to the following angle [27]:

$$\gamma = \arcsin(\alpha_{max}).$$

This is consistent with the definition that is, if $|\theta_j(0) - \theta_i(0)| \leq \gamma$ for all nodes in $\mathcal{C}$, then $|\theta_j(t) - \theta_i(t)| \leq \gamma$ for all nodes in $\mathcal{C}$ and any future time t. An amazing thing that can be understood from this definition is that, if the angle γ decreases then the collective behaviour within the cluster gets more coherent and cohesive, while the weights on connections raise [27].

Kuramoto model in neural hubs, modules and regions

After the discussions in the last subsections on the importance of network architecture and the phenomenon of clustering in neural networks, we have understood that the connection pattern plays an important role in synchrony and dysynchrony and relative convergence rates. From graph theory, we already know that the connection between each pair of nodes is represented

by an edge between them. In the context of neural networks, this is identical to the neural wiring between two neurons. This means that the topological structure of the wiring lattice in neural networks is certainly an important object of study to measure the strength of neural connections. It has been hypothesized that the high-degree regions (hubs), commonly referred to as "rich clubs", facilitate neuronal intermodular interactions and subsequently influence the brain's processing ability, such as vision, hearing, motor functions, and overall whole-body functions.This frequency is related to synchronization phenomena, where neuronal dynamics and their relationship to complex structural pathways can be studied using synchronization dynamic models to understand cluster dynamics and community formation of neuronal subpopulations. The existence of neuronal functional subsystems and high degree nodes within a large-scale network is suggested. Observational experiments on the brains of mammals such as cats, macaques and humans have shown that these so-called high-degree nodes are found in almost all functional areas, underpinning their important role in neuronal communication [28]. Here, the Kuramoto model is used as a prominent synchronization model to simulate neuronal synchrony in terms of structural communication (wiring) and its functional derivation in cross-domain interactions such as inter- and intra-modular activities.

Here, we briefly convey some ideas of the synchronization effects of structurally connected [29] networks by disrupting the intrinsic oscillatory behaviour of the brain regions in the cortical network of the brain. This idea may contribute to unravelling the effects of structural brain pathways on brain functions. To this end, some neural nodes were selected from brain imaging experiments [28] based on the degree of connectivity. Here also the Kuramoto model as a potent paradigmatic model for oscillatory synchronizations can be exploited to simulate the dynamics of group-averaged anatomical brain networks with constant random natural frequencies and some initial phases.As we have already seen, the Kuramoto model can be used here as a :

$$\dot{\theta}_i = \omega_i + \lambda \sum_{j=1}^{N} W_{ij} \sin(\theta_j - \theta_i),$$

where λ is the cortical edge-coupling strength and W_{ij} is the $(i,j)^{th}$ input of the adjacent matrix of the network. Here, the oscillators were assigned a random initial phase from the interval $[-\pi, \pi]$ for each run of the above system, together with an interval frequency that is evenly distributed over $[0, 1]$. The innovative idea here is that there are two order parameters r and r_{link} that describe the global coherence. The simple parameter, r , is based on the previous idea of the equation:

$$z(t) = \frac{1}{N} \sum_{j=1}^{N} e^{i\theta_j(t)} = r(t)e^{i\Phi(t)},$$

where $z(t)$ is a complex number $(z \in \mathbb{C})$. Furthermore, since the main focus is on measuring the level of synchrony within a network, it might be instructive to derive a new index, called *average-edge-wise synchrony*, which provides information about the (pathway) state of the network [28]. This index can be defined as follows:

$$C_{ij} = \frac{1}{\Delta t} \left(\sum_{\tau}^{\tau+\Delta t} e^{i(\theta_i(t) - \theta_j(t))} \right).$$

Measurement of edge synchrony between the i^{th} and j^{th} nodes. The entire data of this index

form C, which is known as *simulated functional connectivity matrix*. The average levels of up-edge synchronization give the *link order parameter*, r_{link}:

$$r_{link} = \frac{1}{N(N-1)} \sum_{i,j} C_{ij},$$

where N is the *total number of node components*. The first order parameter of phase coherence, r, and this new order parameter for fractionally synchronized nodes together describe the global dynamics of the system. To go a little beyond the analysis of the global dynamics, it might be helpful to investigate the synchronization dynamics on a modular scale, i.e. to analyse the nodes in terms of their functional modules. To investigate the possibility that certain nodes are synchronous, they should be classified into synchronized or non-synchronized clusters. Therefore, the value r_{link}, ranging from zero, which corresponds to a *completely incoherent* state, to one, which corresponds to *complete coherence*, can be used to determine the proportion of synchronized nodes. By considering a threshold for synchronization, C_{ij}, it may be useful to reform the definition of overall coherence and incoherence in terms of $(N(N-1) \times r_{link})$ equals perfectly coherent and $(N(N-1) \times (1-r_{link}))$ completely incoherent nodes described by a binary synchronization matrix $[F_{ij}]$ [28]:

$$F_{ij} = \begin{cases} lr1, & N(N-1)r_{link} \; large \; elements \; of \; the \; C_{ij}, \\ 0, & lower \; values \; of \; C_{ij}. \end{cases}$$

By averaging the F_{ij} values for $n = 10^3$ numerical trials of each λ values, (repetition of the trials), we obtain [28]:

$$r_{ij} = \frac{1}{n} \sum_{l=1}^{n} F_{ij}(l),$$

where r_{ij} is the probability that regions i and j are synchronized and l is the trial number. According to this notion of the probability of synchronization between two regions, the modular synchronization $r_{\alpha\beta}$ is determined as follows:

$$r_{\alpha\beta} = \frac{1}{N_\alpha N_\beta} \sum_{i\in\alpha, j\in\beta} r_{ij},$$

where α and β represent the two modules and N_α and N_β are the number of nodes in each of the two areas. Extending the scale to the intra-modular synchronization $\alpha = \beta$, the last equation changes to the following equations:

$$r_{\alpha\alpha} = \frac{1}{N_\alpha(N_\alpha - 1)} \sum_{i,j\neq i\in\alpha} r_{ij},$$

where any node has been set as the pivot of synchronization with the rest of the nodes within the module. If we return to the mean-field representation, which is a suitable approach for inter-modular and inter-hub synchronization, we can change the Kuramoto model of the system back

to:

$$\dot{\theta_k} = \omega_k - R_k \sin(\phi_k - \theta_k),$$

where the assumption is:

$$R_k e^{i\phi_k} = \frac{1}{D_k} \sum_j W_{kj} e^{i\theta_j}.$$

Here R_k is the *radius* and ϕ_k the *phase* of the centroid of the node k and D_k is the *degree of connectivity* for node k. It might be insightful to divide the equation into modules' contribution to the mean-field that allows us to measure the strength of each module's influence on the frequency of node k [28]:

$$\frac{1}{D_k} \sum_j W_{kj} e^{i\theta_j} = \frac{1}{D_k} \left(\sum_{j\in\alpha} W_{kj} e^{i\theta_j} + \sum_{j\in\beta} W_{kj} e^{i\theta_j} + ... \right) = \frac{1}{D_k} \left(D_{k,\alpha} R_{k,\alpha} e^{i\phi_{k,\alpha}} + D_{k,\beta} R_{k,\beta} e^{i\phi_{k,\beta}} + ... \right),$$

where similarly $D_{k,\alpha}$ is the index of connectivity of node k and module α, $R_{k,\alpha}$ stands for the amount of influence that module α contributes to the frequency of node k, and $\phi_{k,\alpha}$ or the *averaged phase* of nodes in module α that are connected to node k. Similar results and expressions can be obtained for relative hubs instead of modules where the equation changes to:

$$R_{k,hubs} e^{i\phi_{k,hubs}} = \frac{1}{D_{k,hubs}} \sum_{j\in hubs} W_{kj} e^{i\theta_j}.$$

It should be considered that this equation only works for $D_{k,\alpha} > 1$ in order to regulate the results. Otherwise, this will not work as a measure of phase coherence. For further details of analysis, and interpretations, please check [28] and [30].

7 Kuramoto model and brain neural disorders

Neural synchrony in brain disorders

There is evidence that brain neural disorders such as epilepsy, Parkinson's disease and Alzheimer's disease are highly associated with abnormal neural synchronization [30]. This may arise through undesired connections or loss of necessary connections. Research suggests the existence of a strong correlation between abnormal synchronization and disorders linked to temporal co-ordinations. This is because of the strong dependence of brain function, specifically cognitive and motor functions, on synchronization activities and neural interactions. Here the main focus of our discussion will be on motor dysfunctions as principal neural disorders that affect many adults.

Parkinson's disease

Parkinson's disease is basically a movement disorder. It is caused by the degeneration of dopaminergic neurons belonging to an area of the brain called *Substantia Nigra*. It is one of the more common neurological disorders, usually appearing in older adults. However, the main recognized causes have not yet been clearly identified. There is some suggestion of genetic causes and indication of causes by toxic impurities. As mentioned, Parkinson's disease onsets when Dopamine neurons, known as Dopaminergic neurons, start to die in Substantia Nigra. The Substantia Nigra is a part of the *Basal Ganglia* which is the central command area of the brain that controls movements and

is connected to the motor cortex. When the dark substance in Substantia Nigra starts to disappear, early symptoms of the Parkinson's disease emerge. The Substantia Nigra can be divided into two sub-areas. One is the *PARS RETICULATA* that receives signals from a part of Basal Ganglia called *STRIATUM*, and sends messages to *Thalamus* via a neurotransmitter called *GABA* (gamma-amino batyric acid). The other part of Substantia Nigra is *PARS COMPACTA*. This is the main area that is damaged when the Parkinson's disease appears. It's role is to dispatch message signals to STRIATUM via the neurotransmitter Dopamine and this communication passes through the *NIGROSTRIATAL* pathway which helps to stimulate the cerebral cortex and onset of movements. Therefore, when responsible neurons in PARS COMPACTA start to die or loose their functionality, the symptoms of low-movements appears that is called *Hypokinetic* in the medical language and is a common symptom of Parkinsonian patients. Motor symptoms of the Parkinson's disease are direct results of excessive synchronizations of neurons mainly belonging to Basal Ganglia. The affected brain of Parkinson's affected patients usually stays on the boundary of synchronized (phase-locked) and desynchronized states, but not on a regular basis of intermittent synchrony similar to a healthy brain [31]. The degeneration of Dopaminergic neurons in Parkinson's disease actually shifts the oscillatory dynamics of the neurons closer to this boundary and triggers motor deficiencies [31]. The most frequent supporting areas of extreme synchronizations in the brain are the feedback circuits of the Basal Ganglia and the membrane features of its neurons. Particularly, β—band frequency oscillations, with frequencies around $20Hz$, are related to motor control where its disfunction appears in Parkinsonian patients. In this case, we can see that the synchronization between Basal Ganglia and cortical communication signals are weakened and results in attenuation of sub-Thalamic nuclei neurons. The strength of these oscillations in the sub-Thalamic nucleus is inversely correlated with motor activities [31].

Symptoms and causes

Commonly observed symptoms of Parkinson's disease are the debilitated motor activities such as inability and slowness of movements, known as *Akinesia*, rigidity of muscles and tremor. Pathophysiological experiments have revealed that the mechanism of initiation for these symptoms are different. However, normally all dysfunctions are related to Basal Ganglia, with the firing rates of neurons in this area being amended and leading to the emergence of a wide variety of movement disabilities. Recent research in neuroscience shows an important correlation between synchronization in β—band oscillations and the Akinesia where an increment in β—band frequency oscillations have been observed within the sub-Thalamic nuclei, GPe and GPi(sub-areas of the Substantia Nigra) of Parkinsonian patients [30]. Figure 5 depicts the excitatory-inhibitory network

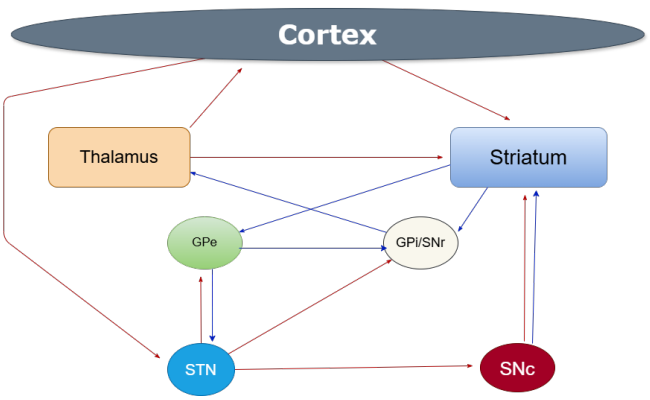

Figure 5. Schematic diagram of excitatory-inhibitory connection pattern in Basal Ganglia (the red and blue arrows are excitatory and inhibitory connections, respectively)

pattern of the basal ganglia. It is hypothesised that suppression of synchronization pattern in $\beta-$band oscillations of cortical motor areas is a main cause of Akinesia. According to this idea, medication therapies aiming to decrease Akinesia focus on reducing synchronization in $\beta-$band and easing $\gamma-$band oscillations. This includes medication treatments aiming to increase the level of Dopamine to compensate for sub-Thalamic nuclei lesioning [30].

Medication and treatment strategies for Parkinson's disease

In recent years, medical science has proposed different ways for treatment and control methods to suppress the potential causes of the Parkinson's disease to some extent and help with Parkinson's disease symptoms. It makes sense that any medication or treatment should increase the Dopamine signalling in order to compensate for the drop-off. The major goal of dopamine-based medications, such as L-DOPA, is to reduce the level of synchrony between sub-Thalamic nuclei and the GPi which is a part of the Basal Ganglia in the range of $\beta-$ frequency [31]. These ideas have some experimental supports although it is not yet agreed that there is a direct link between them. *AMANTADINE* is a medication that increases endogenous Dopamine secretion. *Levodopa* which is the predecessor of the Dopamine that has the ability to cross the blood brain barriers whereas the Dopamine can not [32, 33]. Levedopa will be converted to Dopamine by an enzyme called *Dopa Decarboxylase* within the nigrostrial neurons, and this will keep the balance of Dopamine within brain, although the progression of Dopamine-based degeneration will not stop completely.

Deep-brain stimulation

A special and popular method for controlling and treatment of the Parkinson's disease is *deep-brain stimulation* (DBS). DBS is basically a special type of implantable electrode system that directly affects the Basal Ganglia via transmitting electrical pulses so as to suppress unfavourable activities within the brain. DBS has been designed in a way to shift the global dynamics of the brain, that is the communication dynamics between various areas towards a healthy condition. One outcome of this approach is the higher level of communication and coherence among responsible neurons during the influence of DBS in comparison to previous state. When DBS is connected to the target areas, the primary goal is to modulate the macroscopic activity of neurons via imposing some sort of stimulation by changing the firing rate of neurons and increasing the occurrence of bursting behaviour [34]. The definition of modulation has been discussed in [6]. The underlying mechanism of DBS is to first identify the functional connectivity [29] in the target area of stimulation within the unhealthy brain, and then to try and map the following changes as a result of this perturbation [35]. Not only does DBS alter the functional connectivity patterns, but it has been observed that structural connectivity [29] will be changed by imposing DBS in long term due to changes in interneuronal synchronization patterns [35]. It was shown that DBS therapy has significant effects on changing the neural activity of neural disorder patients. As a result, it was observed that sub-thalamic nucleus DBS therapy can reverse the cortico-thalamic couplings. In addition, DBS can also reduce the level of excessive connections among NAc neurons and the prefrontal cortex by stopping the low-frequency oscillations of the neurons in this area. Key is that DBS tries to re-balance the functional and structural network activities of patient's brain, but still the exact mechanism of how it really affects the whole brain neural networks remains unclear. In [36], it was shown that the overall effective-connectivity of motor-cortico-striatal and thalamo-cortical neural transmission pathways will improve after DBS therapy. In other research, exploiting fast-recording methods such as EEG, it was observed that the extreme synchronization on $\beta-$band frequency among sensorimotor neurons and the sub-thalamic nucleus in Parkinsonian brain will substantially decrease and restore after DBS therapy, supporting the notion that therapeutic DBS is beneficial and effective in improving motor symptoms of Parkinsonian patients [37, 38]. Note that a healthy

brain should remain on the border of a critical dynamics. This idea corresponds to the critical-parameter value in the language of dynamical systems. Thus, when mathematically speaking, it might be helpful to analyse the DBS behaviour and its substantial effects on the brain through this viewpoint. In [35] a bifurcation analysis of DBS effects on the brain activity of Parkinsonian patients has been carried out. To this end, the authors have translated the concept of criticality onto an equivalent mathematical definition in terms of the *edge of bifurcation*. Then behaviour changes can be considered as the transitions between the two sub-areas of the bifurcation diagram. Using this approach we can explore the dynamics of DBS impacts on brain functions both globally and locally. First, the authors traced the functional connectivity of different areas of the brain at resting-state for Parkinsonian patients with DBS being ON and OFF. Amongst various techniques for evaluating empirical and simulated data of functional connectivity such *ks-d* or *static fitting*, the Kuramoto order parameter emerges. This can be used to capture the variation of the brain system's oscillation across the set time-scale as in Eq. (4), where the phases are in fact the phases of BOLD signals. However, due to coping with a physiological signal rather than an artificial signal, some filtering techniques are required.

Disadvantages and side effects of DBS

Although DBS is proven to be beneficial for suppressing symptoms of Parkinson's disease, it has objectionable side effects too. The most common side effects are speech disorders, balance issues and sleep problems [39]. Of most concern are the long-term effect of DBS on neural activities, damage to the tissue and disruption of regular neural activities. A practical disadvantage of DBS is the need for battery replacements and recharging. This is because DBS therapy for regions such as sub-thalamic nucleus and GPi requires high frequency stimulations that consumes high amounts of energy. Battery replacement is only possible via highly-risky neurosurgical operation. In [34], there is a comprehensive discussion on computational models for neural activities, such as the famous Hodgkin-Huxley model as a foundation for conductance activity, and optimization methods both mathematically and technically for modelling the interactions of DBS therapy and its fundamental alterations on neural oscillations and proposing CLDBS (closed-loop DBS) plus alternative signalling approaches and target selection has been done. In the next part we introduce a new idea for improving the set-up of the DBS and optimizing its performance.

Adaptive deep-brain stimulation

A further modification of DBS is *adaptive deep-brain stimulation* (aDBS). Here, the neural activity of selected areas of the brain are modulated within a feedback-controlled framework. In [39] they have suggested a special Kuramoto-type model which allows to incorporate three crucial features of Parkinsonian brain's neural activity. The advantage of aDBS compared to DBS is that it can automatically adjust stimulation parameters providing large-scale energy supply, plus more accurate target selections [39]. Also, it can be considered as a brain-computer interface due to the feedback-loop nature of BCIs. Their generalized form Eq. (2) of the Kuramoto model was proposed as a neurobiological-based model for Parkinson's disease. The specific modification that incorporates the distance-dependent transmission delay is:

$$\dot{\theta}_i = \omega_i + \frac{K}{N}\sum_{j=1}^{N} \cos(\alpha_{ji}) \sin(\theta_j - \theta_i),$$

where α_{ji} is the realistic delay term. To enhance this model for Parkinson's disease, three characteristics including *spatial*,*temporal* and *frequency features* should be employed. For spatial features,

the α_{ji} term can determine the excitatory-inhibitory nature of interactions and connectivities [39]. These considerations allow design of DBS via finding the most effective place for DBS electrodes to reduce distance effects. In case of frequency characteristics the ω_0 of the Kuramoto model can be sampled from a non-symmetric distribution rather than classic symmetric distribution set-up. This results in plausible PSD shape of local field potentials to compare healthy and unhealthy conditions. Also, the shape of signals can be changed via specific considerations to optimize the model and provide more realistic behaviour. A comprehensive analysis of various frequency configurations and the subsequent results of DBS implications can be found in [34].

Epilepsy and seizure disorder

Epilepsy, or epileptic seizure, is a common neurological disorder with a long history of medical research stretching back to ancient Greece. According to the ILAE, epilepsy is a chronic condition of the brain where sustained generation of seizure is triggered when neurons have irregular, or more precisely, incorrect signal propagation [40, 41]. In epilepsy, neurons may synchronise when they are not meant to, while voltage-gated ionic activities [11] do not act regularly. Moreover, electrical impulsing processes are subject to severe disturbance, and neurotransmitters lose control on opening and closing of channels, leading to a chaotic excitatory-inhibitory regime. Extreme excitations or insufficient inhibitions result in *paroxysmal*. These neuronal breakdowns are manifested physically as involuntary movements, or often as a loss of awareness and emotional disorders [40]. In contrast to Parkinson's disease with its long-lasting symptoms, epilepsy, as a collection of multiple but temporary issues, is considered a disorder [41].

Causes of epilepsy

There are six major causes of epileptic disorders [42]: (i) genetics; (ii) structural; (iii) metabolic; (iv) infections; (v) immune; and (vi) unknown reasons. The three main symptoms of epilepsy are *seizure* [42]: (i) focal; (ii) generalized; and (iii) unknown. A detailed, clinical analysis of epileptic seizure can be found in [42]. The infection distribution of epilepsy across age has a bimodal structure, with prevalence in two major age-groups – infants and older adults over 50, specifically adults over 70 [42]. In addition to age reasons, sometimes other incidences may also cause epileptic disorders. As an example, head trauma, tumours or cerebrovascular disease can also trigger the onset of epilepsy [42].

Neural mechanisms and effects

The exact neurological mechanisms that cause epileptic seizures are still unclear. However, onset of abnormal activities is primarily in the cortical areas (focal epileptic seizures) and secondarily in the ganglial neurons [42]. Depending on the region of epileptogenesis, seizures may cause different disorders. Seizures restricted to parts of the cortex, usually causing focal epilepsy, lead to cognitive and motor symptoms. If hallucinations take place, then the sensory areas of the brain will be affected, while if motor areas are affected, then myoclonia can be observed [30]. In the case of convulsive seizures, a majority of the neocortex, including subcortical areas, will undergo abnormal synchronization. For non-motor seizures, thalamo-cortico-thalamic networks will generate low-frequency, highly synchronous oscillations that cause damage to the cognitive functions [30]. In summary, excessive synchronization in neuronal interactions has a large role in the emergence of epileptic disorders, linking back to syncrhonisation phenomena in Kuramoto models.

Kuramoto modelling of epileptic seizure

In recent years, significant experimental research has been conducted to find clinical, biological and surgical treatments for control and suppression of epileptic seizures and symptoms. Mostly they seek to manage pathological conditions, especially unfavourable synchronization of neurons. Initially, anti-seizure medications are used to suppress these conditions, However, after some time, epileptic patients became drug-resistant and these methods are not effective any more. In parallel to these experimental approaches, theoretical approaches have looked to model the possibility of preventing undesired synchronous activities of epileptic brains. Here, we briefly review two such approaches that focus on the Kuramoto model.

The first approach focuses on topological locations of reverse coupling, so called *contrarian nodes*. These simulate the brain's pacemaker local behaviour [43] as the driver nodes so as to investigate the feasibility of preventing unfavourable synchrony. The dynamics of the contrarian nodes (neurons) in terms of the Kuramoto model are [43]:

$$\dot{\theta}_i = \omega_i + K \sum_{j=1}^{N} \mathcal{A}_{ij} \sin(\theta_j - \theta_i - \tau),$$

where the phase shift term τ can be set $\tau = \pi$. This set up means $\sin(\theta_j - \theta_i - \pi) = -\sin(\theta_j - \theta i)$ and the Kuramoto model dynamics of the whole system will be divided into two equations for regular, resp. contrarian, nodes:

$$\begin{cases} \dot{\theta}_i &= \omega_i + K \sum_{j=1}^{N} \mathcal{A}_{ij} \sin(\theta_j - \theta_i) \quad \text{(regular nodes)}, \\ \dot{\theta}_i &= \omega_i - K \sum_{j=1}^{N} \mathcal{A}_{ij} \sin(\theta_j - \theta_i) \quad \text{(contrarian nodes)}. \end{cases}$$

Here the matrix of connections $\mathcal{A}$ follows a Baraba'si-albert network type [44] so as to be realistic to brain neural networks. Varying the coupling strength K for contrarian nodes changes the level of effect on target dysynchronisation. So applying the idea of contrarian nodes opens up the possibility affecting synchrony [43]. Regarding the topology of the network, the contrarian nodes were considered in three configurations. First, as driver nodes, second as high-degree nodes with equal number to driver nodes and finally randomly selected. In all configurations, the observed dynamics of the system obey the proposed model [43]. Comprehensive numerical simulations are discussed in [43].

In terms of synchronization modelling, seizure can be considered as an example of excessive synchronization propagation through the brain neural network. The brain's pacemakers (contrarians) can be placed in selected areas to impose electrical stimulations to restore the healthy conditions. Deep-brain stimulation as a potential option can interfere by transmitting low voltage impulses to disrupt the excessive synchronization and prevent the appearance of seizures. Similar to Parkinson's disease, it is still unclear which parts of the brain are the most effective targets for stimulation so as to bring the highest level of accuracy in controlling the symptoms. The potential of the Kuramoto model here is that the suggested generalization of the Kuramoto model enables us to track the excitatory-inhibitory behaviour of neurons. This is because the coupling strength can determine the level of impact that each neuron has on its adjacent neurons and the sign of coupling determines the excitatory (positive coupling) or inhibitory (negative coupling) impacts. Exploiting neuroimaging techniques, in addition to theoretical studies, it was shown that the interaction of contrarian nodes with their close neighbours is effective for suppression of excessive synchronous behaviour, and prevention of seizure [43]. So, by assigning a pacemaker role to each node, we can explore various possible outcomes of desynchronization targets. The Kuramoto

order parameter can be used to measure the level of coherence in these different topological structures resulting from contrarian nodes.
The second approach is to consider non-constant, time-varying coupling. Here K follows a logistic growth, aiming to better resemble epileptic seizure activity. Then the Kuramoto model can be used to study the replication of epileptic seizures according to its synchronous behaviour whilst neurons generate action potentials that result in epileptic seizure [41]. The focus is on the most extreme state of epilepsy, called *status epilepticus*, that is induced by a special procedure called *Lithium-pilocarpine* – a common method to induce seizures and *epilepticus* in animal brains particularly mice and rat. The purpose of this approach is to develop treatments. The motivation for the use of a logistic growth model is that it enables an S-shaped evolution of the seizure [45]. Immediately after injection of *pilocarpine* (a cholinergic muscarinic agonist that stimulates cholinergic neurons) the seizure level increases quickly, but then slowly settles to a steady state. After this stage, the first symptoms of seizure appear in the animal's behaviour [45]. The logistic dynamics for K are incorporated in to the Kuramoto model as follows: [45]:

$$\begin{cases} \dot{\theta}_i = \omega_i + \frac{K}{N}\sum_{j=1}^{N}\sin(\theta_j - \theta_i), \\ \dot{K} = aK(1 - \frac{K}{C}), \end{cases}$$

where a is the *growth rate* and C is the *the carrying capacity* [22]. The order parameter for this modified model is given by [45]:

$$r = \frac{1}{N}\sqrt{\left(\sum_{i=1}^{N}\cos(\theta_i)\right)^2 + \left(\sum_{i=1}^{N}\sin(\theta_i)\right)^2}, \quad i \in \{1, 2, 3, ..., N\}.$$

Subsequently, the critical value of the coupling term is given by:

$$K_c = \frac{N(\omega_{max} - \omega_{min})}{2\big(\sin(\gamma) + (N-2)\sin(\frac{\gamma}{2})\big)},$$

where

$$\gamma = 2\arccos\left(\frac{-(N-2) + \sqrt{(N-2)^2 + 32}}{8}\right).$$

According to previous discussions, we know that whenever the coupling exceeds this critical value, synchronization appears and the incoherent state becomes unstable due to synchronization (partially). Below K_c, there is no special synchrony while epileptic seizure will emerge after exceeding of K_c. Numerical analysis and simulations for this modified Kuramoto model are discussed in detail in [45]. This new modelling idea may suggest insights on drug-therapy for epileptic seizures.

8 Discussion and conclusion

This review has presented the Kuramoto model as a fundamental model for exploring different aspects of neural activities, from both mathematical and biological perspectives. Starting with a comprehensive mathematical analysis, it was shown that the model is a robust framework for neural activities, providing a solid foundation for synchronous neural interactions. The application of the model to a wide range of neural processes, particularly its flexibility to reshape

or simulate complex brain functions and dysfunctions, was demonstrated in terms of its ability to replicate relative strategies to control and suppress symptoms of disorders. Altogether, these stages highlight the Kuramoto model's ability as both a precise mathematical object and as a model for developing therapies through connecting theoretical and computational insights. We have tried to provide the reader (especially early-career researchers) with integrated material for potential research ideas in the area of brain studies with a logical hierarchy consisting of mathematical, phenomenological, and clinical viewpoints. Further attempts should focus on finding more advanced forms of the Kuramoto model such as controllable models, delayed models that can represent the dynamics of neural responses, or learning types of Kuramoto to improve its predictive and practical abilities for medical and neuroscientific inquiries.

9 Potential implications

In this review, our aim was to gather insights on the applications of the Kuramoto model in brain cortical activities and highlight the interesting ideas from various aspects on how the Kuramoto model can assist us to represent and simulate each neural synchronization process. However, many open problems remain unanswered that readers may study in future works. As an example, finding an explicit form of the Kuramoto model that can represent the dynamics of a disordered brain is still a challenge. In recent studies the main focus was on model development for therapeutic strategies rather than introducing an exact form of the Kuramoto model that only demonstrates the (dys)synchronization patterns taking place when the brain is afflicted by a neural disorder. Although the probable reasons for these disorders and the underlying synchronization and desynchronization phenomena are in hand, the explicit form of the Kuramoto model that can justify the behaviour of a particular disease has not been suggested yet. Another area that has attracted the attention of multidisciplinary research activities is to develop control strategies for suppression of symptoms based on the Kuramoto model. Here, we reviewed two examples – adaptive deep brain stimulation and logistic coupling for the Kuramoto model. But we still face many questions on how we can improve these ideas to make them more applicable for clinical implications. It may sound a little idealistic to propose a model that has the capability to be applied in real-time treatments, but ultimately we need to optimize the results of theoretical research for applications in real-world trials and subsequently actual treatments of mentioned disorders.
Following this proposal, the authors of this review are currently working on the restoration of healthy activity in a Parkinson-diseased brain. The core idea of our research is to first qualitatively analyse the dynamics of neurons particularly in basal ganglia before and after the appearance of Parkinson's disease. Then, based on the data we have acquired (e.g., EEG signals), we try to design a set of artificial neural networks (ANN) founded on the basis of the Kuramoto model. Our terminology consists of two special words for the ANNs, the healthy brain, which represents the dynamics of a non-Parkinsonian brain called healthy neural network (HNN), and the other one is the damaged neural network (DNN) representative of the afflicted areas of the brain. DNN should be a subsystem of HNN showing areas of the brain that suffer from disorder. The next step is to exploit deep-brain stimulation and develop feedback control strategies to suppress the disease. Deep-brain stimulation will insert impulses according to the input data obtained from the DNN, and analysed by the HNN. So, with the help of adaptive control strategies for deep-brain stimulation plus the assistance of the Kuramoto model, we hope to identify the optimal stimulation targets, and approximate stimulation parameter range to excite the DNN and so recover as much as possible of its healthy condition.

Nomenclature

Table 1. List of Abbreviations

Abbreviation	Meaning
BOLD	Blood oxygenation Level Dependent
CLDBS	Closed-loop Deep-brain Stimulation
DBS	Deep-brain Stimulation
EEG	Electroencephalogram
GPCR	G-protein-coupled Receptorl
GPi/GPe	Globus Pallidus (Internal/External)
ILAE	International League Against Epilepsy
L-DOPA	Levodopa
LGIC	Ligand-gated Ion Channels
ODE	Ordinary Differential Equation

Declarations

Use of AI tools

The authors declare that they have not used Artificial Intelligence (AI) tools in the creation of this article.

Data availability statement

All data generated or analyzed during this study are included in this article.

Ethical approval

The authors state that this research complies with ethical standards. This research does not involve either human participants or animals.

Consent for publication

Not applicable

Conflicts of interest

The authors declare that they have no conflict of interest.

Funding

This article was funded by the University of Exeter research funding scheme.

Author's contributions

All authors discussed the results and contributed to the final manuscript equally.

Acknowledgements

The authors would like to thank the anonymous reviewers for their helpful comments and feedback, which greatly strengthened the overall manuscript.

References

[1] Winfree, A.T. Biological rhythms and the behavior of populations of coupled oscillators. *Journal of Theoretical Biology*, 16(1), 15-42, (1967). [CrossRef]

[2] Strogatz, S.H. From Kuramoto to Crawford: exploring the onset of synchronization in populations of coupled oscillators. *Physica D: Nonlinear Phenomena*, 143(1-4), 1-20, (2000). [CrossRef]

[3] Kuramoto, Y. Self-entrainment of a population of coupled non-linear oscillators. In Proceedings, *International Symposium on Mathematical Problems in Theoretical Physics*, pp. 420-422, Kyoto, Japan, (1975, January). [CrossRef]

[4] Kuramoto, Y. Chemical turbulence. In, *Chemical Oscillations, Waves, and Turbulence* (pp.111-140). Springer, Berlin, Heidelberg: Springer, (1984). [CrossRef]

[5] Strogatz, S.H. Kuramoto Model. *Nonlinear Dynamics and Chaos: with Applications to Physics*. CRC Press: New York, (2024).

[6] Pikovsky, A., Rosenblum, M. and Kurths, J. *Synchronization: A Universal Concept in Nonlinear Sciences*. Cambridge University Press: Cambridge, (2001).

[7] Ott, E. and Antonsen, T.M. Low dimensional behavior of large systems of globally coupled oscillators. *Chaos: An Interdisciplinary Journal of Nonlinear Science,* 18(3), 037113, (2008). [CrossRef]

[8] Ott, E. and Antonsen, T.M. Long time evolution of phase oscillator systems. *Chaos: An Interdisciplinary Journal of Nonlinear Science,* 19(2), 023117, (2009). [CrossRef]

[9] Zou, W. and Wang, J. Dynamics of the generalized Kuramoto model with nonlinear coupling: Bifurcation and stability. *Physical Review E,* 102, 012219, (2020). [CrossRef]

[10] Barioni, A.E.D. and de Aguiar, M.A. Complexity reduction in the 3D Kuramoto model. *Chaos, Solitons & Fractals,* 149, 111090, (2021). [CrossRef]

[11] Ermentrout, B. and Terman, D.H. *Mathematical Foundations of Neuroscience* (Vol. 35). Springer: New York, (2010). [CrossRef]

[12] Lovinger, D.M. Communication networks in the brain: neurons, receptors, neurotransmitters, and alcohol. *Alcohol Research & Health,* 31(3), 196-214, (2008).

[13] Rodrigues, F.A., Peron, T.K.D., Ji, P. and Kurths, J. The Kuramoto model in complex networks. *Physics Reports,* 610, 1-98, (2016). [CrossRef]

[14] Acebrón, J.A., Bonilla, L.L., Pérez Vicente, C.J., Ritort, F. and Spigler, R. The Kuramoto model: A simple paradigm for synchronization phenomena. *Reviews of Modern Physics,* 77, 137-185, (2005). [CrossRef]

[15] Bag, B.C., Petrosyan, K.G. and Hu, C.K. Influence of noise on the synchronization of the stochastic Kuramoto model. *Physical Review E,* 76(5), 056210, (2007). [CrossRef]

[16] Peng, J. *Synchronization in the Second-Order Kuramoto Model*. Ph.D. Thesis, Department of Mathematisch, The University of Humboldt-Universität zu Berlin, (2015). [https://edoc.hu-berlin.de/items/49909278-f5ba-4835-a004-c8b27cafc1a4]

[17] Sakagushi, H. Cooperative phenomena in coupled oscillator systems under external fields. *Progress of Theoretical Physics,* 79(1), 39-46, (1988). [CrossRef]

[18] Barreto, E., Hunt, B., Ott, E. and So, P. Synchronization in networks of networks: The onset of coherent collective behavior in systems of interacting populations of heterogeneous oscillators. *Physical Review E,* 77, 036107, (2008). [CrossRef]

[19] Montbrió, E. and Pazó, D. Kuramoto model for excitation-inhibition-based oscillations. *Physical Review Letters,* 120(24), 244101, (2018). [CrossRef]

[20] Izhikevich, E.M. *Dynamical Systems in Neuroscience*. MIT Press: United States, (2007).

[21] Kuroki, S. and Mizuseki, K. Excitation–inhibition balance controls synchronization in a simple model of coupled phase oscillators. *Neural Computation,* 37(7), 1353-1372, (2025). [CrossRef]

[22] Kuznetsov, Y.A. *Elements of Applied Bifurcation Theory* (Vol. 112). Springer: New York, (1998). [CrossRef]

[23] Frolov, N. and Hramov, A. Extreme synchronization events in a Kuramoto model: The interplay between resource constraints and explosive transitions. *Chaos: An Interdisciplinary Journal of Nonlinear Science,* 31(6), 063103, (2021). [CrossRef]

[24] Cumin, D. and Unsworth, C. Generalising the Kuramoto model for the study of neuronal synchronisation in the brain. *Physica D: Nonlinear Phenomena,* 226(2), 181-196, (2007). [CrossRef]

[25] Ferrari, F.A.S., Viana, R.L., Lopes, S.R. and Stoop, R. Phase synchronization of coupled bursting neurons and the generalized Kuramoto model. *Neural Networks,* 66, 107-118, (2015). [CrossRef]

[26] Novikov, A.V. and Benderskaya, E.N. Oscillatory neural networks based on the Kuramoto model for cluster analysis. *Pattern Recognition and Image Analysis,* 24, 365-371, (2014). [CrossRef]

[27] Favaretto, C., Cenedese, A. and Pasqualetti, F. Cluster synchronization in networks of Kuramoto oscillators. *IFAC-PapersOnLine,* 50(1), 2433-2438, (2017). [CrossRef]

[28] Schmidt, R., LaFleur, K.J., de Reus, M.A., van den Berg, L.H. and van den Heuvel, M.P. Kuramoto model simulation of neural hubs and dynamic synchrony in the human cerebral connectome. *BMC Neuroscience,* 16, 54, (2015). [CrossRef]

[29] Avena-Koenigsberger, A., Misic, B. and Sporns, O. Communication dynamics in complex brain networks. *Nature Reviews Neuroscience,* 19, 17-33, (2018). [CrossRef]

[30] Uhlhaas, P.J. and Singer, W. Neural synchrony in brain disorders: relevance for cognitive dysfunctions and pathophysiology. *Neuron,* 52(1), 155-168, (2006). [CrossRef]

[31] Rubchinsky, L.L., Park, C. and Worth, R.M. Intermittent neural synchronization in Parkinson's disease. *Nonlinear Dynamics,* 68, 329-346, (2012). [CrossRef]

[32] Bauer, D.C. and McPhee, S.J. *Pathophysiology of Disease: An Introduction to Clinical Medicine*. McGraw-Hill Education: New York, (2013).

[33] Jameson, J.L., Fauci, A.S., Kasper, D.L., Hauser, S.L., Longo, D.L. and Loscalzo, J. *Harrison's Principles of Internal Medicine*. McGraw-Hill: New York, (2018).

[34] Yu, Y., Wang, X., Wang, Q. and Wang, Q. A review of computational modeling and deep brain stimulation: applications to Parkinson's disease. *Applied Mathematics and Mechanics,* 41, 1747-1768, (2020). [CrossRef]

[35] Saenger, V.M., Kahan, J., Foltynie, T., Friston, K., Aziz, T.Z., Green, A.L. et al. Uncovering the underlying mechanisms and whole-brain dynamics of deep brain stimulation for Parkinson's disease. *Scientific Reports,* 7, 9882, (2017). [CrossRef]

[36] Kahan, J., Urner, M., Moran, R., Flandin, G., Marreiros, A., Mancini, L. et al. Resting state functional MRI in Parkinson's disease: the impact of deep brain stimulation on 'effective' connectivity. *Brain,* 137(4), 1130-1144, (2014). [CrossRef]

[37] Ray, N.J., Jenkinson, N., Wang, S., Holland, P., Brittain, J.S., Joint, C. et al. Local field potential beta activity in the subthalamic nucleus of patients with Parkinson's disease is associated with improvements in bradykinesia after dopamine and deep brain stimulation. *Experimental Neurology,* 213(1), 108-113, (2008). [CrossRef]

[38] Weinberger, M., Mahant, N., Hutchison, W.D., Lozano, A.M., Moro, E., Hodaie, M. et al. Beta oscillatory activity in the subthalamic nucleus and its relation to dopaminergic response in

Parkinson's disease. *Journal of Neurophysiology*, 96(6), 3248-3256, (2006). [CrossRef]

[39] Kuzmina, E., Dylov, D.V. and Lebedev, M. Advanced modeling for adaptive DBS: Capturing Parkinson's disease complexity. In Proceedings, *2024 8th Scientific School Dynamics of Complex Networks and their Applications (DCNA)*, pp. 150-153, Kaliningrad, Russian, (2024, September). [CrossRef]

[40] Engel, J. *Seizures and Epilepsy* (Vol. 83). Oxford University Press: New York, (2013).

[41] Fisher, R.S., Acevedo, C., Arzimanoglou, A., Bogacz, A., Cross, J.H., Elger, C.E. et al. ILAE official report: a practical clinical definition of epilepsy. *Epilepsia*, 55(4), 475-482, (2014). [CrossRef]

[42] Thijs, R.D., Surges, R., O'Brien, T.J. and Sander, J.W. Epilepsy in adults. *The Lancet*, 393(10172), 689-701, (2019).

[43] Mohseni, A., Gharibzadeh, S. and Bakouie, F. The role of driver nodes in managing epileptic seizures: Application of Kuramoto model. *Journal of Theoretical Biology*, 419, 108-115, (2017). [CrossRef]

[44] Estrada, E. and Knight, P.A. *A First Course in Network Theory*. Oxford University Press: USA, (2015).

[45] Zavaleta-Viveros, J.A., Toledo, P., Avendaño-Garrido, M.L., Escalante-Martínez, J.E., López-Meraz, M.L. and Ramos-Riera, K.P. A modification to the Kuramoto model to simulate epileptic seizures as synchronization. *Journal of Mathematical Biology*, 87, 9, (2023). [CrossRef]

Bulletin of Biomathematics (BBM)
(https://dergipark.org.tr/en/pub/bulletinbiomath)

How to cite this article: Dabbaghchi, A. & Townley, S. (2025). Around the brain in 80 Hz: A Kuramoto model perspective of cortical neuronal activity. *Bulletin of Biomathematics*, 3(2), 111-149. https://doi.org/10.59292/bulletinbiomath.1664603